



UNIVERSITÀ DEGLI STUDI DI TRENTO

FACOLTÀ DI SCIENZE MATEMATICHE FISICHE E NATURALI

SCUOLA DI DOTTORATO IN FISICA (23° CICLO)

INVESTIGATIONS OF BIOLOGICAL MEMBRANES BY NMR AND ESI-MS METHODOLOGIES

DOCTOR OF PHILOSOPHY IN PHYSICS

BY

TOMMASO SANDRON

SUPERVISOR: PROF. GRAZIANO GUELLA

December 2010

To my parents

Contents

1	Introduction	7
1.1	Lipidomics	7
1.2	Detergent Resistant Membranes	14
1.3	Cold resistance in insects larvae	16
2	Analytical methodologies in lipidomics	21
2.1	Basic theory of NMR spectroscopy	21
2.2	NMR experiment	23
2.3	Debye model	27
2.4	Solid-state NMR	28
2.5	ESI mass spectrometry	30
2.5.1	Phosphocholine lipids	34
2.5.2	Phosphoethanolamine lipids	36
3	Material and methods	39
3.1	Materials	39
3.2	Mixture of standard lipids	39
3.3	DRMs and whole cell membranes isolation and extraction . .	40
3.4	FAME preparation and GC-MS analysis	40
3.5	Stress protocol and lipid extraction from larvae	41
3.6	LC-MS Measurements	42
3.7	NMR Measurements	43

CONTENTS

4	Results and discussion	45
4.1	Standard mixture of lipids	45
4.2	Lipid profile of PSMA-anchoring rafts	51
4.3	Cold resistance in Chironomid larvae	61
4.3.1	<i>Diamesa cinerella</i>	62
4.3.2	<i>Pseudodiamesa branickii</i>	73
4.3.3	Discussion	80
5	Conclusions	87

Chapter 1

Introduction

1.1 Lipidomics

System biology is the computational integration of genetic, transcriptomic, proteomic and metabolomic information with the intent of understanding all of the molecular processes within a cell organism. The sequencing of the human genome, the development of gene arrays and the availability of soft-ionization mass spectrometry techniques have led the way for high-throughput genomics and proteomics [1]. The end product of genetic and protein expression is the metabolome (see figure 1.1), the total component of metabolites within a cell organism, reflecting the most downstream effects of gene and protein regulation and providing relevant information about the biological state of the system [2]. Metabolomics represents a paradigm shift from looking at individual metabolites to examining complete metabolic networks in an entire cell or organism.

Within the big area of metabolomics, in the last ten years there has been a new reappraisal of the function of lipids in the cell life, not only with a structural role as cell wall or an energy storage function, but also with a significant function on signaling and protein recognition processes (see figure 1.2). This new attention on lipids has led to a new research field in the metabolomics world called Lipidomics [3]. Lipidomics is more than just the

Introduction

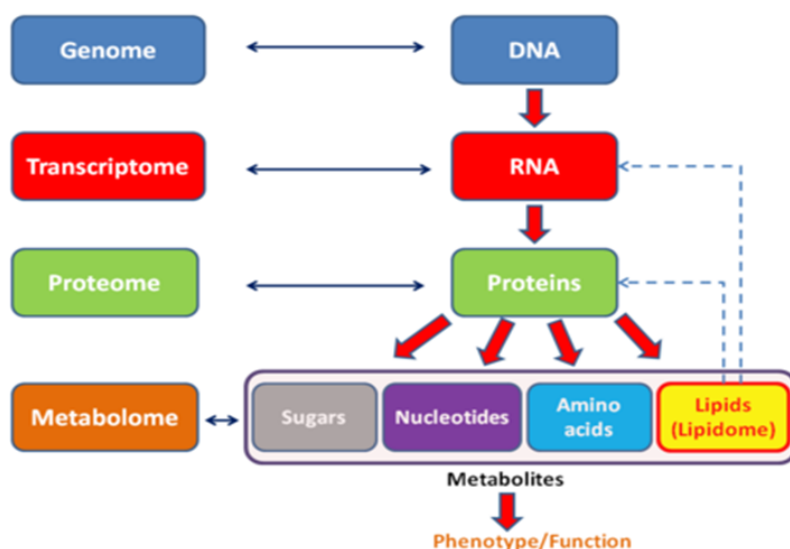


Figure 1.1: The "omics" world from gene to metabolite

complete characterization of all lipids in a particular biological sample. It is the comprehensive understanding of the influence of all lipids on a biological system with respect to cell signaling, membrane architecture, transcriptional and translational modulation, cell-cell and cell-protein interaction and response to environmental changes over time. The critical role of lipids in cell, tissue and organ physiology is demonstrated by many human diseases involving the disruption of lipid metabolic enzymes and pathways. Examples of such diseases include diabetes, cancer, neurodegenerative disorders and infectious diseases. This warrants the expectation that clinical diagnosis of these diseases will greatly take advantage from lipid pattern analysis and represents a clue for understanding the molecular diversity observed in membrane phospholipids. Subtle biophysical properties are also another possible explanation of strong interest toward lipids especially with reference to the emerging field of heterogeneous membrane microdomains (rafts). The major goal in lipidomics is the identification of metabolic pathways which are activated or deactivated during development of an organism or when a cell is shifted from an established physiological condition to an-

1.1 Lipidomics

other physiological or pathological condition (metabolic learning). A better understanding of the regulation of underlying metabolic pathways is necessary to design novel strategies for intervention.

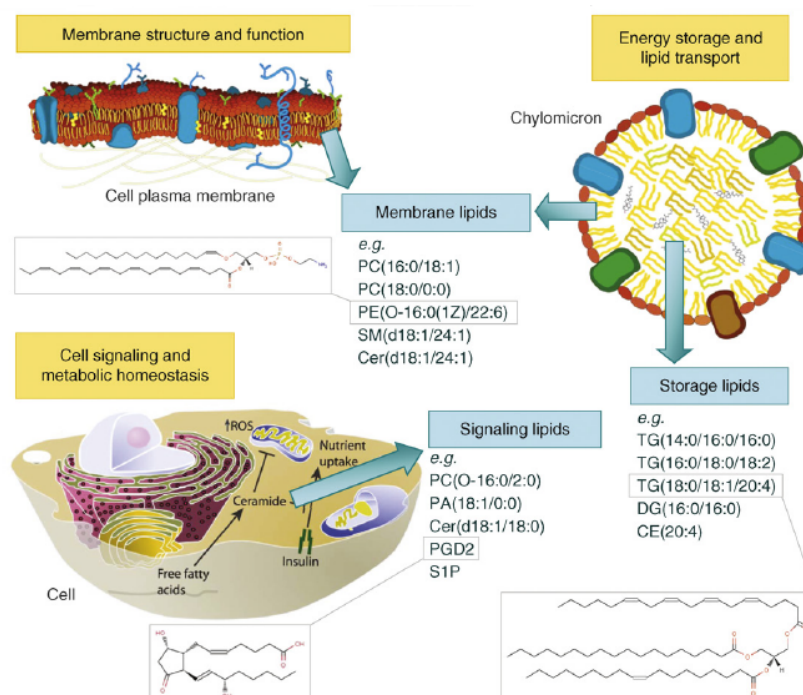


Figure 1.2: Diverse biological roles of lipids, with a few common representative molecular species listed. Reprinted from [4]

Even at present time, lipids are defined as molecules soluble in organic solvents or at least extracted from aqueous systems by use of an immiscible solvent; there are so many examples of lipid substances that do not obey this simple rule that defining these substances based on their biosynthetic origin is much more descriptive [5]; thus a new nomenclature has been proposed for lipids, classifying them into eight major categories: fatty acyls, glycerolipids, glycerophospholipids, sphingolipids, sterol lipids, prenol lipids, saccharolipids and polyketides. This classification shows us the extraordinary large number of lipids in nature. In our work attention has been mainly focused on glycerophospholipids, sphingolipids and cholesterol. The

Introduction

main feature of these polar lipids is their amphipathic property, required to fulfill their primary function in membrane. This amphipathicity is related to their molecular division into a non polar domains (hydrocarbon chains) and polar domains in contact with aqueous solutions; these features are well represented in phospholipids, the most common membrane lipids.

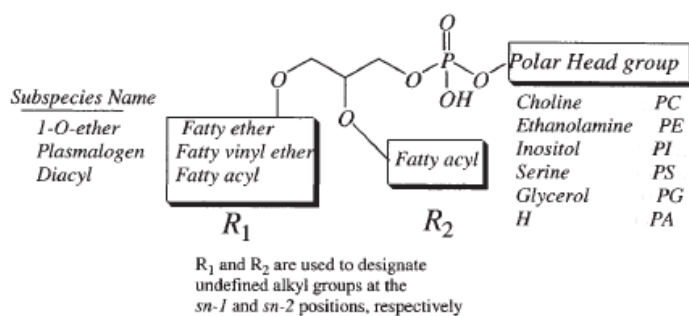


Figure 1.3: Basic structure of a phospholipid

Within the PL class (figure 1.3), glycerol backbone is acylated with long-chain fatty acids at *sn*-1 and *sn*-2 position and in some molecular species the acyl bond can be substituted by an ether or vinyl ether bond. The *sn*-3 position is esterified by a phosphate group, to which is attached a base (choline, ethanolamine), polyol (glycerol, inositol) or amino acid (serine). This group forms the polar part of the molecule. PL have a characteristic chemical nature that determines their inherent self-assembly into bilayer structured membranes. Another class, usually present in membranes, are sphingolipids, based on ceramide which is comprised of a long-chain base, sphingosine, to which a long-chain fatty acid is attached by an amide bond. The most common are sphingomyelins, characterized by the presence of a phosphatidylcholine, called SM-PC (figure 1.4). Sphingolipids differ from most biological phospholipids in containing long, largely saturated acyl chains. This allows them to readily pack tightly together, a property that gives sphingolipids much higher melting temperatures (T_m) than membrane (glycero) phospholipids, which are rich in kinked unsaturated acyl

chains.

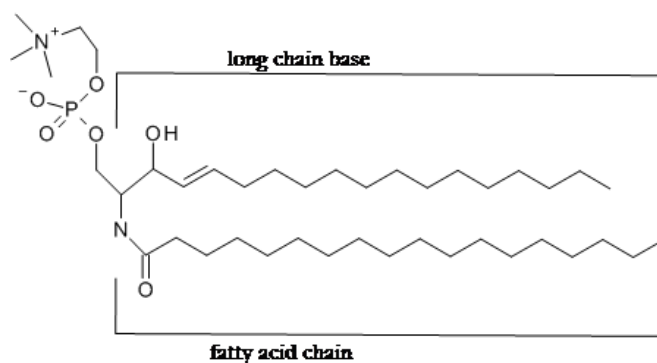


Figure 1.4: Structure of a sphingomyelin

Another important lipid, present mainly in eukaryotic membranes, is cholesterol (figure 1.5). Cholesterol is largely hydrophobic. But it has one polar group, a hydroxyl, making it amphipathic. Cholesterol, an important constituent of cell membranes, has a rigid ring system and a short branched hydrocarbon tail.

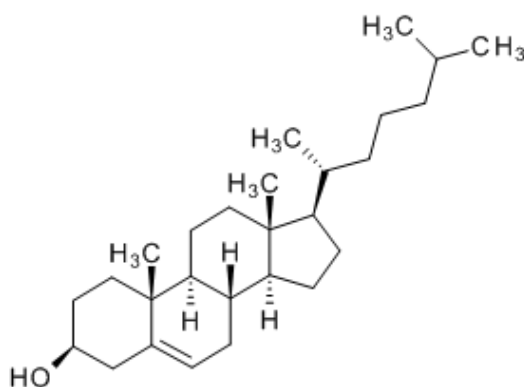


Figure 1.5: Structure of cholesterol

Cholesterol or closely related sterols are major lipid components of the plasma membranes of most eukaryotic cells, and are also found in lower

Introduction

concentrations in many intracellular membranes. Cholesterol has numerous different functions in eukaryotic cells, one of its primary roles being to modulate the physical properties of the plasma membrane phospholipid bilayer. Cholesterol incorporation into bilayers has four effects: first, it broadens and eventually eliminates the cooperative gel to liquid crystalline phase transition of phospholipid bilayers; second, it decreases (increases) the area per molecule of the liquid crystalline (gel) state monolayers; third, it increases (decreases) the orientational order of the hydrocarbon chains of liquid crystalline (gel) bilayers; and fourth, it decreases (increases) the passive permeability of phospholipid bilayers above (below) their gel to liquid crystalline phase transition temperatures. The largest contribution to cholesterol-phospholipid interactions appears to derive from van der Waals and hydrophobic forces, although hydrogen bonding to the polar headgroup and interfacial regions of the host lipid bilayer may be of considerable importance, especially in the sphingolipids and anionic phospholipids.

The rapid growth of lipidomics has primarily resulted from technological advances in mass spectrometry (MS) and the analysis of lipids has been performed by a diverse variety of approaches reflecting the diverse chemical subclasses. Gas chromatography (GC and GC/MS) approaches provide a rapid and sensitive method of analysis. However, in this approach the lipid sample has to be hydrolyzed prior to analysis and the resulting free fatty acids (FFA) have to be converted into the corresponding trimethylsilyl or methyl esters to enhance their volatility. Therefore, the information on the fatty acid prime location is lost. A great improvement to metabolomics and, specifically, to lipidomics has been made by the development of soft-ionization mass spectrometry techniques like ESI-MS [6] and MALDI [7], the former also coupled to an high pressure liquid chromatographic system (HPLC-MS). An example of the great potential of these techniques on lipidomics is the recently work by Ejsing et al. [8], where they have mapped the global composition of lipid component of *Saccharomyces cerevisiae*. Furthermore MALDI has permitted to make experiments not only on extracts

but also on samples simply obtained from whole cells, tissues or organisms [9]. These mass spectrometric techniques are useful thanks to their high resolution and sensitivity and to the ability to profile complex mixtures in a straightforward way. There are also some disadvantages: the necessity (for ESI) of samples prepared by preliminary extraction procedures, the difficulties in quantitative analyses due to the MS response factors of the phospholipids classes [10] requiring to provide reliable working curves and/or internal standards.

Another powerful technique that has contributed to the development of lipidomics allowing to obtain quantitative and qualitative informations has been high-resolution NMR. It allows structure elucidation, qualitative and quantitative analysis of defined molecules and even complex mixtures. Not all nuclei are accessible to the NMR-experiment. But those which are important in lipid chemistry like 1H , ^{13}C , and ^{31}P are recordable as a matter of routine with modern instruments equipped with multinuclear transmitter-probes. The drawbacks are the low sensitivity intrinsic of this technique, the need of extraction procedures and the use of detergents to resolve all signals in a ^{31}P NMR spectrum, hindering a final recovery of the sample. To overcome these problems, in recent years, another NMR technique has been applied to metabolomic/lipidomics investigations that permits to make measurements directly on cell or tissues: solid state NMR.

In addition to LC-MS and NMR, another physical techniques have been applied in lipidomics: infrared and Raman spectroscopy. These techniques allow to perform analysis on ex-vivo samples, avoiding extraction procedures, and to identify possible markers of diseases [11] also with the coupling with microscopic techniques. These techniques, however, are not able to distinguish the various phospholipid classes or to separate contribution due to triglycerides and to phospholipids because they give informations only about the lipid conformational order, the acyl chain packing order or the mean unsaturation degree, all global data and not specific to a single class or lipid.

Introduction

In this thesis attention has been focused on two biological systems to demonstrate how the study of membrane lipids can help for a better understanding of the mechanisms involved in different biochemical processes. In the first example we have studied the components of DRM (detergent resistant membrane) associated with the expression of PSMA, a protein involved in the prostate carcinoma. In the second we have analyzed the composition of membranes of two insect larvae of two species (*Pseudodiamesa branickii* and *Diamesa cinerella*) to obtain information about the mechanisms involved in the adaptation of the organisms at temperatures below 0 °C.

1.2 Detergent Resistant Membranes

The fluid mosaic model [12] was the principal model used to describe membrane structure until two decades ago. Instead, it is now known that lipids are distributed asymmetrically between the outer and inner leaflets of the bilayer [13] and that this imposes a different organization of membrane components on the lateral axis. According to this, the disparity between various lipid populations results in the separation of liquid and gel-like phases within one membrane. The gel-like phase consists of small membrane entities, which can move easily in the fluid remainder of the membrane. These dynamic structures are called lipid rafts (or lipid microdomains, membrane microdomains, DRMs) [14]. The single universal physicochemical attribute of membrane microdomains is their ability to resist extraction with non-ionic detergents (for example, Triton X-100) at 4°C [15]. This initial demonstration of the existence of DRMs in cells has now become a widely established and adopted method for their isolation from biological samples and has led to the term "Detergent Resistant Microdomains, DRMs" [16] which encompasses several membrane populations that share the common ability to remain insoluble in various detergents. Their resistance to detergents is, in turn, related reciprocally to their composition, as reported

1.2 Detergent Resistant Membranes

in a work by Schuck and coworkers [17]. These microdomains exist in a liquid-ordered (l_o) phase, an intermediate state between the conventionally named L_β and L_α states that have also been designated solid-ordered (s_o) and liquid-disordered (l_d) respectively, and they are dispersed into the liquid-disordered phase of the lipid bilayer. This new phase is related to its composition, formed principally by cholesterol and sphingolipids. The first has the ability, in a liquid crystalline phase, to order acyl chains decreasing the area per molecule and inducing the segregation of liquid ordered domains; sphingolipids favor this segregation process because they have more saturated chains optimizing acyl chain packing [18]. Acyl chains of lipids in the (l_o) phase are extended and tightly packed, as in the gel phase, but have a high degree of lateral mobility [15]. Two general models have emerged to explain the relative stability of lipid rafts [19]. One centers on the role of headgroup interactions and hydrogen bonding [20] [21]. In one form [14], it is posited that sphingolipids interact with each other through their headgroups and through the interaction of the amide of the sphingosine base of one sphingolipid with hydroxyls or carboxyls of an adjacent sphingolipid. In that case, many sphingolipids would associate through the formation of a network of bonds [22]. The cholesterol would effectively pack into the space between the sphingolipids in a manner analogous to the way it fills space between phospholipids. Hydrogen bonding between the 3-OH group of cholesterol and the amide of the sphingosine would stabilize this localization of cholesterol. The other model [23] considers the interactions between the chains as the primary determinant. This model places emphasis on the fact that saturated acyl chains are more extended than unsaturated ones and pack well with each other into liquid-ordered phases [24]. Cholesterol may interact more favorably with a saturated than an unsaturated sphingolipid because cholesterol is a flat, rigid molecule. The interactions between acyl chains of the sphingolipids and cholesterol would be the critical factor in creating rafts.

DRM are involved in the recognition and transport process of the prostate

Introduction

specific membrane antigen (PSMA) [25], a 750-residue type II transmembrane glycoprotein of the normal prostate cells and one of the most promising biomarkers of prostate carcinoma [26] as its expression is drastically increased in cancer cells protein involved in the prostate carcinoma [27]. In particular, the complex glycosylated form of the protein is found in Lubrol insoluble DRMs. Many essential cellular events, such as protein sorting, endocytosis and signal transduction pathways, are triggered via association of the proteins directly implicated in these processes with DRMs. The aim of this work is to determine the lipidic profile of these microdomains, in particular to establish the quali-quantitative changes in lipid distribution between DRM and whole cell membrane of the cancer cell line. We have focused the attention on two factors: the molar ratio between cholesterol and phosphatidylcholine (PC) and the relative molar ratio of the various between the various phospholipid classes (PC, SM, PE). In order to gain this information we analyzed the samples by NMR (1H and ^{31}P) and HPLC/ESI-MS.

1.3 Cold resistance in insects larvae

Membrane is the main part used by cell to communicate with the outside, to transport molecules inside and outside it and to preserve its integrity and life against abiotic and biotic stresses. In physiological conditions membrane is in a liquid-crystalline phase characterized by a certain degree of disorder, mobility and fluidity and these features have to be maintained to preserve the integrity of the cell. The main process accessible to the cell to conserve membrane fluidity, in case of low temperature adaptation, is the lowering of the transition temperature from gel to liquid phase, also called melting temperature (T_m) modifying the membrane composition [28]. This lowering can be obtained with many processes, among which the increase of unsaturation degree of the fatty acid chain of phospholipids, the increase of expression of some proteins (antifreeze proteins and heat shock proteins)

1.3 Cold resistance in insects larvae

and the binding of little molecules (sugars, glycerol) to the membrane.

It has been demonstrated, in literature, that the insertion of unsaturated chains in phospholipids (both PC and PE) lowers the melting temperature of the membrane [29][30] varying, for example, from 82.5 °C for a 20:0/20:0 PE model bilayer to 3.5 °C for a 20:0/20:5 PE bilayer [31]. The trend of melting temperature with temperature could be described, at first approach, by a simple model based on these assumptions: 1) the monoenoic sn-2-acyl chain in the sn-1-saturated/sn-2-monounsaturated phospholipid molecule is assumed to adopt, at $T < T_m$, an energy-minimized crankshaft-like motif in the gel state bilayer; hence, it consists of a longer chain segment and a shorter chain segment separated by the cis double bond; 2) the longer segment and the neighboring all-trans sn-1-acyl chain run in a parallel manner with favorable van der Waals attractive distance between them; 3) the shorter segment is considered to be partially disordered at $T < T_m$, analogous to the molten polypeptide chain of proteins, thus playing a relatively insignificant role in the attractive van der Waals chain-chain interactions in the gel state bilayer; 4) the sn-2-acyl chain containing two cis double bonds is highly flexible in the gel state bilayer, leading to a weakest lateral chain-chain interaction in comparison with other sn-1-saturated/sn-2-polyunsaturated lipids; 5) when the sn-2-acyl chain contains three or more cis double bonds, however, these methylene-interrupted cis double bonds can be considered as an essentially immobile unit in the gel state bilayer.

The use of small molecules (sugars, polyols) as cryoprotectants is one of the most used methods by invertebrates and plants, in particular trehalose and glycerol [32][33][34]. It has been shown that the molecular mechanism underlying this cryo-protective effect is the hydrogen bonding pattern of the trehalose molecules to the bilayer headgroups [35]. The sugar can "substitute" some of the hydrogen bonds normally provided by water and by that stabilize the fragile bilayer arrangement. Stabilization or destabilization here mean that the bilayer is able to withstand harsher or less harsh conditions in presence of small molecules compared to the pure bilayer in water.

Introduction

Trehalose is experimentally known to prevent the lipid from undergoing a phase transition under cooling, i.e., it shifts the main phase transition temperature significantly [36].

Knowledge as to how aquatic insects will potentially react and adapt in face of increasing human impacts is one of the major challenge in prediction of future freshwater biodiversity trends. One main driver of biodiversity change has been individuated, global warming. In relation to this driver, one adaptive trait was selected, resistance to adverse temperature conditions, in two target insect species (Diptera: Chironomidae): the cold stenothermal and stenotope *Pseudodiamesa branickii* (Nowicki) and *Diamesa cinerella* (Meigen). These species are frequent in cold mountain springs and streams (<7-8 °C). These species, as reported in literature [37], have developed a complex of strategies to survive at their physiological temperature minimum, comprising morphological, behavioral, ecological, physiological and biochemical adaptations. The first three adaptations have been deeply discussed [38], whereas the last two only recently have been investigated, highlighting the role of cryo-protectants and anti-freezers molecules (polyols, sugars and proteins) [39][40]. Five candidate genes have been indicated as determinants for resistance to cold and warm temperature (hsc70, hsp70, hsp90, afps). Heat shock proteins are known to be involved in temperature variation resistance in many organisms, as well as antifreeze proteins in cold resistance.

The general aim of this project is to give new insights on how these aquatic organisms could respond to the oncoming temperature increase related to global climate change. This by the i) characterization of genetic determinants of resistance to abiotic stresses in natural populations of the two selected target species and ii) definition of the role of metabolites such as proteins and sugars and of the membrane lipid composition in development of such resistances.

This work is inserted in a bigger study on biodiversity with the aim to study the direct consequences that biodiversity changes or loss may involve

1.3 Cold resistance in insects larvae

in the ecosystem and the selected ecological, genetic and biochemical mechanisms implemented by living organisms to adapt to environmental stresses.

Introduction

Chapter 2

Analytical methodologies in lipidomics

2.1 Basic theory of NMR spectroscopy

NMR spectroscopy was developed in '50s observing the interaction between the magnetic component of radiation and the magnetic dipoles associated to angular momentum of nuclei. Angular momentum of nuclei is related to a magnetic momentum by the constant γ , defined as gyromagnetic ratio

$$\mu_z = \gamma l_z = \gamma M_l \hbar \quad (2.1)$$

μ_z is z component of magnetic momentum, l_z z component of angular momentum and M_l is quantic number related to angular orbitalic momentum. In solution, with good approximation, we can consider only the spin component of magnetic momentum, defined by the quantic number I. If we consider only nuclei with I = 1/2, we have only two value for $M_l = \pm 1/2$, representing two different spin states, autofunctions of operator \hat{I}_z : $|\alpha\rangle$ state and $|\beta\rangle$ state, with respective autovalues +1/2 and -1/2. These states have the same energy with zero field, but, if we applied a static magnetic field, the states are splitted to two different energies due to Zeeman interaction between magnetic field and nuclear magnetic dipoles. This interaction can

Analytical methodologies in lipidomics

be expressed by a spin hamiltonian

$$\hat{H}_{Ze} = -\gamma\hbar\hat{I}_zB_0 \quad (2.2)$$

From equation 2.2 we can calculate autoenergies of the two spin states

$$E_\alpha = \langle\alpha|H|\alpha\rangle = -\frac{1}{2}\gamma\hbar B_0 \quad (2.3)$$

$$E_\beta = \langle\beta|H|\beta\rangle = \frac{1}{2}\gamma\hbar B_0 \quad (2.4)$$

In figure 2.1 the energy splitting due to Zeeman interaction is schematically drawn.

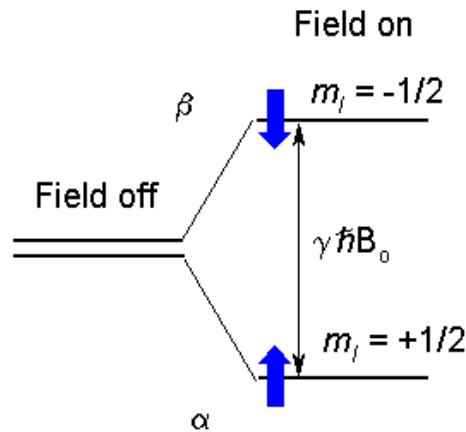


Figure 2.1: Energy splitting of spin states due to Zeeman interaction

The response of the spin of the overall magnetization to an applied magnetic field is to move around the field, like in figure 2.2; this motion is called precession.

The spin rotate around magnetic field with a frequency of precession that is equal to

$$\omega_0 = -\gamma B_0 \quad (2.5)$$

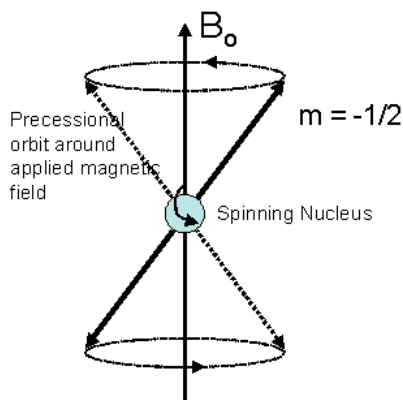


Figure 2.2: Precession of magnetization around magnetic field

where B_0 is the magnetic field applied and γ is the gyromagnetic ratio. In NMR ω_0 is called Larmor frequency and it's also related to the transition energy between two spin states $\Delta E = \hbar\omega_0$. The sense of spin precession depends on the sign of γ . Most nuclei have positive γ , with a consequent negative Larmor frequency; in this case the precession is in the clockwise direction.

2.2 NMR experiment

At equilibrium, once applied the static magnetic field along z-axis, we have only longitudinal magnetization that is undetectable. To observe signal, we have to distort the equilibrium magnetization and the simplest method to do this is to apply an additional magnetic field $B_1(t)$ perpendicular to B_0 to excite spin transitions; in this way we obtain a transverse magnetization that is observable, as we can observe in figure 2.3. Normally the additional magnetic field is applied as a radiofrequency pulse with an appropriate power, frequency and duration.

The transverse magnetization is observed as a complex signal, called FID

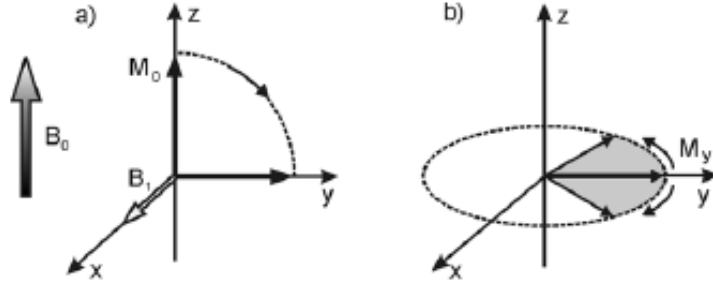


Figure 2.3: Effect of the application of a rf pulse on magnetization

(Free induction decay), that could be divided in two parts: one real and one complex, expressed in equation 2.6

$$f(t) = f_c(t) + if_s(t) \quad (2.6)$$

$$f_c(t) = \cos(\Delta\omega t) \exp(-t/T_2^*) \quad (2.7)$$

$$f_s(t) = \sin(\Delta\omega t) \exp(-t/T_2^*) \quad (2.8)$$

$$f(t) = \exp(i\Delta\omega t) \exp(-t/T_2^*) \quad (2.9)$$

where $\Delta\omega = \omega_0 - \omega$ is the offset frequency and T_2^* (overall transverse relaxation time) includes contributions from field inhomogeneity of the sample (T_2') and from transverse relaxation (T_2).

$$1/T_2^* = 1/T_2 + 1/T_2' \quad (2.10)$$

Converting from time domain to frequency domain by Fourier transform, we obtain a signal with the form of a lorentzian curve with a full width at half-height equal to $\Delta\nu_{1/2} = 1/\pi T_2^*$

$$F(\omega) = \int f(t) \exp(-i\omega t) dt = \frac{\lambda}{\lambda^2 + (\omega - \omega_0)^2} \quad (2.11)$$

2.2 NMR experiment

As seen above, if we obtain a good field homogeneity along the sample by a good shimming, the principal contribution to linewidth is the transverse relaxation. This relaxation is due to molecular motions creating some fluctuating magnetic fields that can be expressed in this way

$$b(t) = |b_0| f(t) \quad (2.12)$$

where $f(t)$ is a function characteristic of the particular motion with these properties: $\overline{f(t)} = 0$ and $\overline{f(t)f^*(t)} \neq 0$. The fluctuations are described by the autocorrelation function $G(\tau) = \overline{f(t)f^*(t+\tau)}$, with these properties: for small τ $G(\tau)$ is always positive and has an high value, for long τ $G(\tau)$ can be positive or negative and is equal to zero for infinite τ , while for τ equal to zero $G(\tau)$ has its maximum value. From these properties we can adopt an exponential form for $G(\tau)$

$$G(\tau) = G(0) \exp(-\tau/\tau_C) \quad (2.13)$$

where τ_C is called rotational correlation time. If we apply Fourier transform to autocorrelation function we obtain the spectral density $J(\omega)$ with the form

$$J(\omega) = \overline{f(t)f^*(t)} \frac{2\tau_C}{1 + \omega^2\tau_C^2} = \frac{2\tau_C}{1 + \omega^2\tau_C^2} \quad (2.14)$$

Generally we can express the velocity of a transition induced by a magnetic field with the formula

$$W = \frac{1}{4} \gamma^2 \left(\frac{1}{2\mu_0} B_{0x}^2 \right) \quad (2.15)$$

In the case of relaxation, where the transitions are induced by the fluctuating fields b , we can rearrange the previous equation in this form

$$W \propto \gamma^2 \overline{b_x^2} J(\omega_0) \quad (2.16)$$

Analytical methodologies in lipidomics

and, for the particular case where the fluctuating fields are due to relaxation, we obtain the following expression

$$W = \frac{1}{T_2} \propto D^2 [AJ(0) + BJ(\omega_0) + CJ(2\omega_0)] \quad (2.17)$$

where D represents the strength of the anisotropic interaction that causes relaxation, and $J(\omega)$ has the form reported in equation 2.14. The last equation shows us the relation between linewidth, related to T_2 , and the rotational correlation time, like described in figure 2.4.

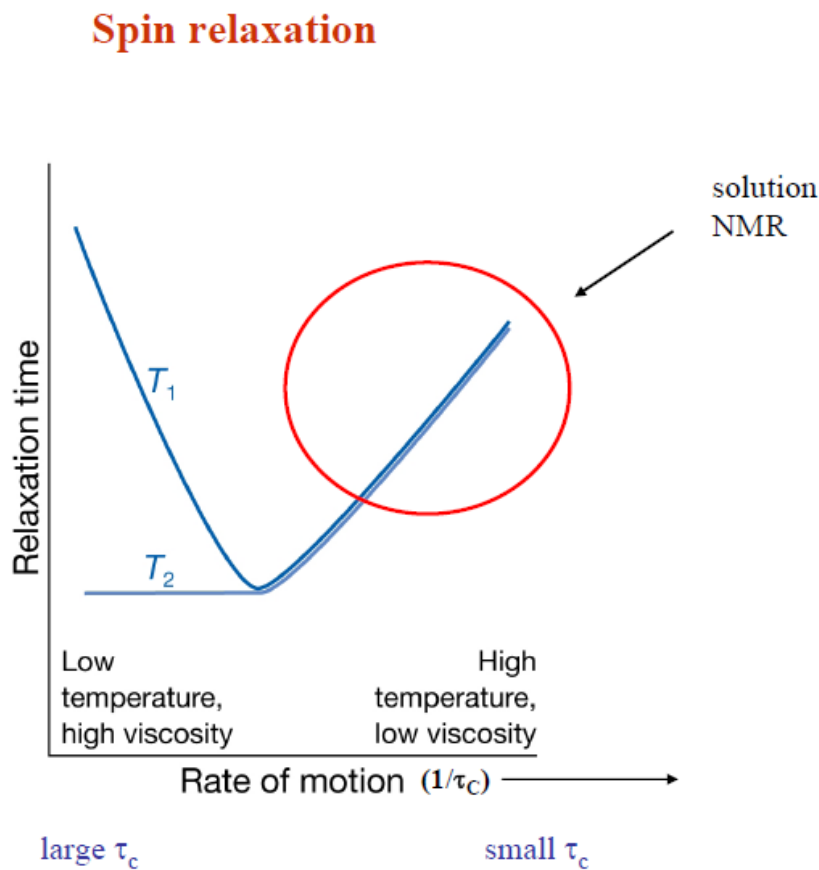


Figure 2.4: Correlation between relaxation time and rotational correlation time τ_C

τ_C depends on some variables like temperature, viscosity of the solvent

and molecular dimensions. The simplest model that describe this relation is Debye model.

2.3 Debye model

The Debye model is the simplest approach to describe rotational molecular diffusion is this: we consider a vector, determining the orientation of the system, that randomly walks around a sphere with an isotropic Brownian motion. We can calculate the vector probability distribution on (θ, ϕ) at time t , starting from the origin $(0,0)$, by the diffusion equation

$$\frac{dP(\theta, \phi, t)}{dt} = D_R \left\{ \frac{1}{\sin\theta} \frac{\partial}{\partial\theta} \left(\sin\theta \frac{\partial}{\partial\theta} \right) + \frac{1}{\sin^2\theta} \frac{\partial^2}{\partial\phi^2} \right\} P(\theta, \phi, t) \quad (2.18)$$

D_R is rotational diffusion coefficient, characteristic of the motion. The equation 2.18 can be solved if $P(\theta, \phi, t)$ is constructed as an expansion of spherical harmonics $Y_{l,m}(\theta, \phi)$

$$P(\theta, \phi, t) = \sum_{l,m} c_{l,m} Y_{l,m}(\theta, \phi) \exp -l(l+1)D_R t \quad (2.19)$$

The correlation time, describing time employed to cover one radiant, could be related to the rotational diffusion coefficient

$$\tau_c = \frac{1}{6D_R} \quad (2.20)$$

Diffusion coefficient is related to the coefficient of friction, f_R , by Einstein equation

$$D_R = \frac{k_B T}{f_R} \quad (2.21)$$

and the coefficient of friction is correlated to molecular parameters by Stoke law

$$f_R = 8\pi\eta r_0^3 \quad (2.22)$$

η is solvent viscosity and r_0 is the molecular hydrodynamic radius approximated to a sphere. Combining two last equations, we obtain Debye equation correlating rotational correlation time to molecular parameters.

$$\tau_c = \frac{4\pi\eta r_0^3}{3k_B T} \quad (2.23)$$

From this model we can deduce that in NMR spectroscopy there is a limit on resolution due to molecular dimensions, i.e. over a certain dimension the linewidth is too large to separate all peaks. To overcome this problem, in the '60s, it has been developed another technique, called Solid-State NMR, allowing to perform NMR experiments on solid and macromolecular samples.

2.4 Solid-state NMR

As we see in the previous section, the spin hamiltonian can be divided in two parts that take account of internal and external contributions.

$$\hat{H} = \hat{H}_{ex} + \hat{H}_{int} = \underbrace{\hat{H}_{Ze} + \hat{H}_{rf}}_{\hat{H}_{ex}} + \underbrace{\hat{H}_{CS} + \hat{H}_Q + \hat{H}_D + \hat{H}_J + \dots}_{\hat{H}_{in}} \quad (2.24)$$

In solids the relative contribution of these interactions is different than in anisotropic or isotropic liquids, as showed in figure 2.5.

From the figure 2.5 we note that the major contributions come from chemical shift, short range dipolar interaction and quadrupolar interaction (only for nuclei with $I \geq 1$). In the general case these contributions overlap resulting in very broad and featureless lines. To reduce the effects of these interactions and to obtain an high resolution solid-state NMR spectrum, some techniques have been developed with the aim of narrowing lines and enhancing signal. The principal techniques, now always used to these

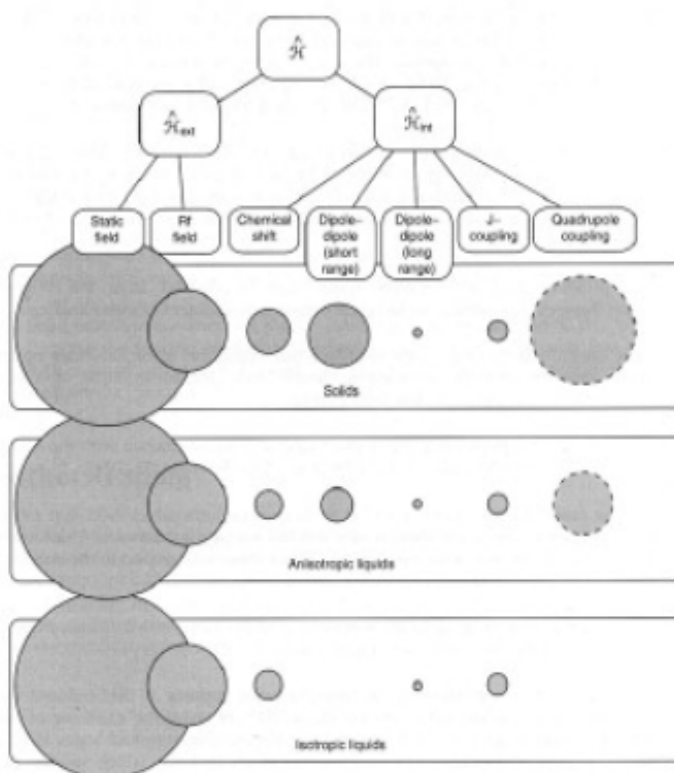


Figure 2.5: Relative magnitudes of the motionally-averaged spin Hamiltonian terms in different phases of matter

Analytical methodologies in lipidomics

aims, are magi-angle spinning (MAS), cross polarization (CP) and spin decoupling.

The two major anisotropic contributions (chemical shift and heteronuclear dipolar coupling), as we can see from the respective hamiltonian 2.25 and 2.26, only if the term $(3\cos^2\theta - 1)$ is equal to zero, i.e. if the angle $\theta=54.7^\circ$; if we spin the sample at this angle we eliminate these contributions and we narrow the lines.

$$\hat{H}_{CS} = \gamma\hbar B_0 I_Z \frac{1}{2} \delta(3\cos^2\theta - 1) \quad (2.25)$$

$$\hat{H}_{D,IS} = \frac{\mu_0}{4\pi} \frac{\gamma_I \gamma_S \hbar^2}{r^3} \frac{1}{2} (3\cos^2\theta - 1) (\hat{I} \cdot \hat{S} - 3\hat{I}_Z \hat{S}_Z) \quad (2.26)$$

MAS is unable to eliminate totally the contribution from heteronuclear dipolar coupling; to do this, we add the effects of heteronuclear decoupling, obtained with multipulse decoupling techniques, less heating the sample than continuous wave decoupling. The other most used technique is the cross polarization that takes advantage of heteronuclear dipolar coupling to transfer polarization from abundant spins (typical 1H) to dilute spins (^{13}C or other).

2.5 ESI mass spectrometry

Mass spectrometry (MS) is an analytical technique that measures the mass-to-charge ratio of charged particles. It is used for determining masses of particles, for determining the elemental composition of a molecule, and for elucidating the chemical structures of molecules, such as peptides and other chemical compounds. The MS principle consists of ionizing chemical compounds to generate charged molecules or molecule fragments and measurement of their mass-to-charge ratios. In a typical MS procedure:

1. A sample is loaded onto the MS instrument, and undergoes vaporization;

2. The components of the sample are ionized by one of a variety of methods (e.g., by impacting them with an electron beam), which results in the formation of charged particles (ions);
3. the ions are separated according to their mass-to-charge ratio in an analyzer by electromagnetic fields;
4. The ions are detected, usually by a quantitative method;
5. The ion signal is processed into mass spectra.

MS instruments consist of three modules:

- An ion source, which can convert gas phase sample molecules into ions (or, in the case of electrospray ionization, move ions that exist in solution into the gas phase);
- A mass analyzer, which sorts the ions by their masses by applying electromagnetic fields;
- A detector, which measures the value of an indicator quantity and thus provides data for calculating the abundances of each ion present

The ion source is the part of the mass spectrometer that ionizes the material under analysis (the analyte). The ions are then transported by magnetic or electric fields to the mass analyzer. A critical step is generating detectable ions from a mixed complex solution. During the last two decades, atmospheric pressure ionization (API) systems have undergone much development and they are now widely utilized in many scientific and technical fields. Their wide spread use is due to their ability to ionize a wide variety of compounds, as well as the complementary information they provide to liquid chromatography. Among API sources, the most popular is the electrospray ionization source [41][42]. It is commonly referred to as "soft source", due to its ability to produce an intense pseudo-molecular parent ion with few fragments, especially in the analysis of polar compounds. It is especially useful

Analytical methodologies in lipidomics

in producing ions from macromolecules because it overcomes the propensity of these molecules to fragment when ionized. Three fundamental processes occur in the ESI-MS, all at atmospheric pressure: aerosol generation, particle ionization and solvent removal from incipient ion.

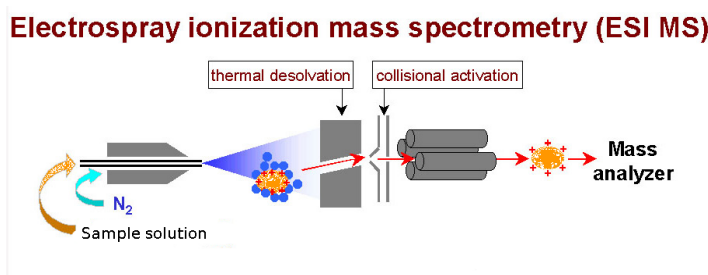


Figure 2.6: A schematic picture of an ESI-MS apparatus with its main parts: a nebulizing source, an ion beam guide and a mass analyzer

During standard electrospray ionization [43], the sample is dissolved in a polar, volatile solvent and pumped through a narrow, stainless steel capillary (75 - 150 micrometers i.d.) at a flow rate of between 1 $\mu\text{L}/\text{min}$ and 1 mL/min. A high voltage of 3 or 4 kV is applied to the tip of the capillary, which is situated within the ionization source of the mass spectrometer, and as a consequence of this strong electric field, the sample emerging from the tip is dispersed into an aerosol of highly charged droplets, a process that is aided by a co-axially introduced nebulizing gas flowing around the outside of the capillary. This gas, usually nitrogen, helps to direct the spray emerging from the capillary tip towards the mass spectrometer. The charged droplets diminish in size by solvent evaporation, assisted by a warm flow of nitrogen known as the drying gas which passes across the front of the ionization source. Droplets with high superficial charge density are produced, and are, thus, dispersed through attraction or repulsion within the electric field. A counter flow of inert heated gas, usually nitrogen, eliminate the residual solvent molecules. This reduces the droplet size until electrostatic repulsion

$$E_c = \frac{V_c}{r_c \ln(4d/r_c)} \quad (2.27)$$

(V_c is the potential difference at capillary-electrode, r_c is the capillary radius, d is the distance between them) overrides the cohesive force of the solvent. There are two major theories that explain the final production of gas-phase ions:

- The Ion Evaporation Model (IEM) [44] suggests that as the droplet reaches a certain radius the field strength at the surface of the droplet becomes large enough to assist the field desorption of solvated ions.
- The Charged Residue Model (CRM) [45] suggests that electrospray droplets undergo evaporation and fission cycles, eventually leading progeny droplets that contain on average one analyte ion or less. The gas-phase ions form after the remaining solvent molecules evaporate, leaving the analyte with the charges that the droplet carried.

Eventually charged sample ions, free from solvent, are released from the droplets, some of which pass through a sampling cone or orifice into an intermediate vacuum region, and from there through a small aperture into the analyzer of the mass spectrometer, which is held under high vacuum. The lens voltages are optimized individually for each sample. The ions observed by mass spectrometry may be quasimolecular ions created by the addition of a proton (a hydrogen ion) and denoted $[M + H]^+$, or of another cation such as sodium ion, $[M + Na]^+$, or the removal of a proton, $[M - H]^-$. The introduction of electrospray ionization mass spectrometry to analyze intact phospholipids has further advanced this area of biochemistry and an additional benefit has come by the coupling of ESI-MS with on-line high-performance liquid chromatography (HPLC) for the separation of phospholipid classes as well as molecular species because it minimizes the exposure of lipids to atmospheric oxygen associated to other chromatographic techniques. Separation of lipids can be accomplished either with normal-phase or reversed-phase HPLC strategies. Normal-phase HPLC separates phospholipids by class on the basis of the head-group polarity. In reversed-phase the separation is based on lipophilicity of individual molecular species; because the elution

sequence is determined by the fatty acyl chains and, therefore, molecular species of different classes likely coelute, some care must be exercised in the analysis of phospholipids. It's very difficult in ESI to obtain absolute quantitative information about composition of a sample, because the degree of ionization of phospholipids varies from one molecular species to another and the instrument response is affected by acyl chain length, unsaturation and lipid concentration [10]. Each phospholipid class has a different ionization and fragmentation mechanism in ESI and in the following paragraphs we discuss the behavior of the two principal classes: PC and PE.

2.5.1 Phosphocholine lipids

Phosphocholine lipids are characterized by the presence of quaternary nitrogen atom whose positive charge is neutralized by the negative charge of phosphate group. The nitrogen atom readily forms an abundant $[M + H]^+$ ion by ESI because the phosphate anion can be easily protonated during the electrospray process. Furthermore, also abundant sodiated ion, $[M + Na]^+$, are observed in positive-ion mode, when sodium ions are present in the electrospray solvent. The first fragment produced by collision-induced decomposition of protonated molecular ion $[M + H]^+$ is the phosphocholine ion at m/z 184 (see figure 2.7), which is typical of all phosphocholine-containing lipids, and is diagnostic for this specific class of phospholipids.

The facile formation of this ion allows us to use precursor-ion scanning of m/z 184 to detect as well as to quantify molecular species of PC lipids present in a complex sample (see figure 2.8, where it's shown the isolation of PC peaks by precursor-ion scanning of m/z 184).

The phosphocholine ion is also present in the fragmentation pattern of sphingomyelin and can be used as marker to detect molecular species of SM lipids. SM can be distinguished from PC because SM molecular ion $[M + H]^+$ has an odd m/z value while PC molecular ion has an even m/z value. In spite of quaternary nitrogen atom with its permanent positive charge also negative ions are formed from PC lipids. The most abundant ions are

2.5 ESI mass spectrometry

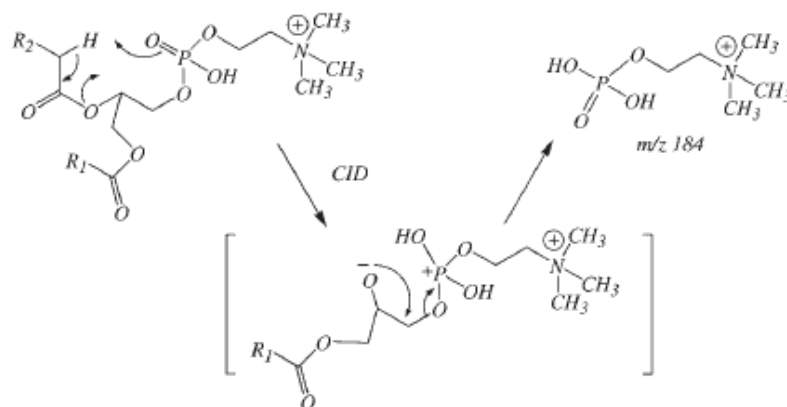


Figure 2.7: Scheme of mechanism for the formation of phosphocholine ion at m/z 184

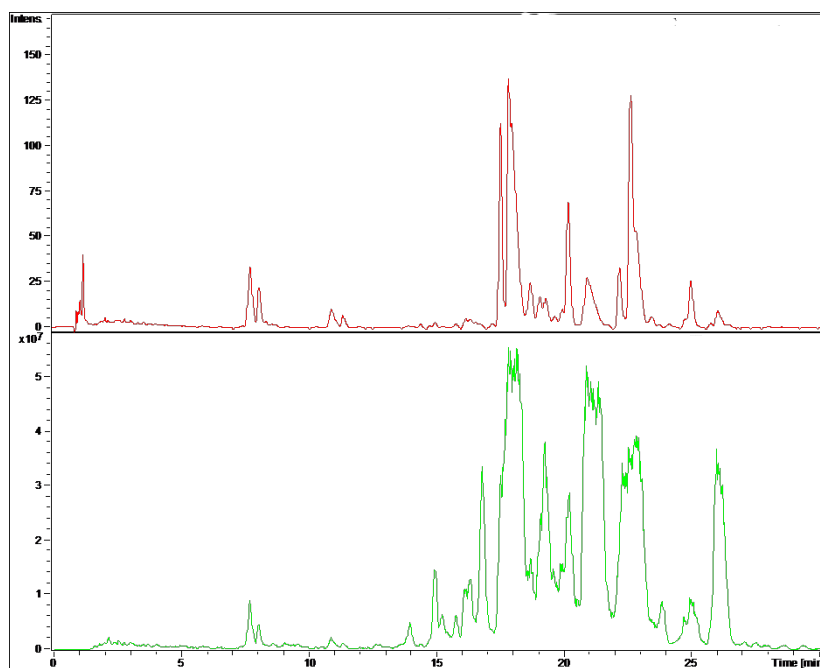


Figure 2.8: LC-MS chromatogram of a lipid sample. Top: UV chromatogram. Bottom: Chromatogram extracted by precursor-ion scanning of m/z 184

$[M-15]^-$, corresponding to the loss of a methyl group from ammonium group, and ions characteristic of the fatty acyl group esterified at the sn-1 and sn-2 position.

2.5.2 Phosphoethanolamine lipids

PE lipids are one of the major class of phospholipids present in cell membranes and in ESI they produce in high abundance positive and negative ions corresponding to $[M+H]^+$ and $[M-H]^-$. The main diagnostic fragment is the ion corresponding to the neutral loss of phosphoethanolamine group (141 U), $[M+H-141]^+$ (see figure 2.9)

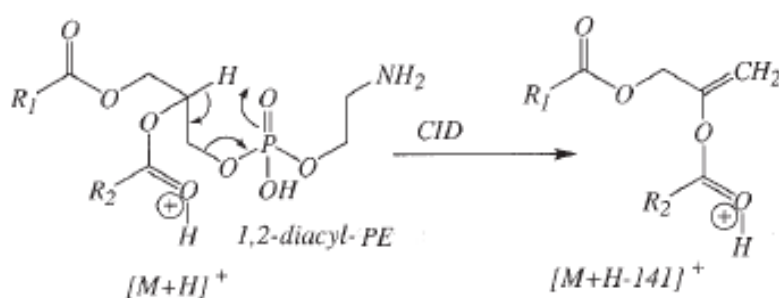


Figure 2.9: Scheme of the formation of $[M+H-141]^+$ ion

In negative-ion mode the characteristic fragments produced from $[M-H]^-$ ion are the carboxylate anions of the fatty acyl chains. These diagnostic ions are well represented in figure 2.10

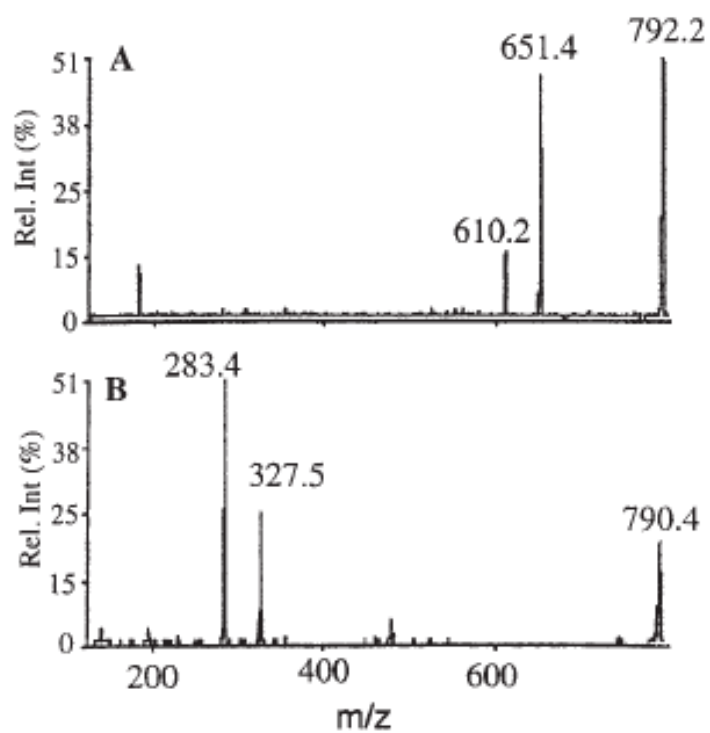


Figure 2.10: Mass spectrometry of phosphoethanolamine lipid in (A) positive-ion mode and (B) negative-ion mode derived from 18:0/22:6 PE. Reprinted from [46]

Chapter 3

Material and methods

3.1 Materials

Synthetic PC, PE, PS, PG, SM, PI and PA were obtained from Avanti Polar Lipids (Alabaster, AL). All solvents were of high performance liquid chromatography (HPLC) or analytical grade and were purchased from Carlo Erba (Milano, Italy), Baker (Deventer, Holland) and Riedel de Haen (Seelze, Germany). Deuterated solvents were purchased from Euriso-top (Gif-sur-Yvette, France) and Aldrich (Steinheim, Germany).

3.2 Mixture of standard lipids

The lipids used to prepare standard mixtures have been: PSPC, DOPE, DOPG, DOPS, SM brain, PI liver and PA egg. All the solution have been prepared in the same solvent ($CHCl_3$) and have the same concentration (5 mg/ml) except PA (10 mg/ml). Two standard lipids mixture have been prepared. For mixture 1 500 μ l of each lipid solution (PSPC, DOPE, DOPG, DOPS, SM brain, PI liver) have been taken and added together. The final solution has been vacuum evaporated to dryness and redissolved in the various solvent systems chosen for ^{31}P NMR experiments: $CDCl_3$, Et_3N / CD_3OD / Na_2EDTA (0.2 M in D_2O) 8/1/1 and $CDCl_3$ / CH_3OH / K_2EDTA

Material and methods

(0.2 M) 8/4/1. For mixture **2** 100 μl of DOPG, DOPE and PSPC solutions and 200 μl of DOPS, SM, PI and PA solutions have been taken and added together. The final solution has been vacuum evaporated to dryness and redissolved in a sodium cholate solution in D_2O (0.9 M).

3.3 DRMs and whole cell membranes isolation and extraction

Lubrol-insoluble DRMs and whole cell membranes were isolated from human lymph node prostate cancer cells (LNCaP). For DRMs extraction, cells were solubilized in Lubrol PX 1 in a cocktail of proteinase inhibitors. After homogenization with a 21-G needle, they were maintained on ice for 2-5 h. Then a first centrifugation (10 min at 1000g) was performed in order to remove cell debris before a second high-speed centrifugation (90 min at 100000g). DRMs were retained in the insoluble pellet. For whole cell membranes extraction, cells were incubated for 30 min in a cocktail of proteinase inhibitors and then homogenized for 1 min at 20000rpm. By a first centrifugation (5 min at 500g) the cell debris was removed. The supernatant was centrifugated (15 min at 10000g) to obtain the heavy membrane fraction. After this centrifugation, the supernatant was centrifugated (60 min at 150000g) to obtain the light membrane fraction. The two fraction (heavy and light) was combined for NMR and LC-MS analysis. Finally lipids extraction from the pellets was carried out according to the method of Bligh and Dyer [47] for both samples.

3.4 FAME preparation and GC-MS analysis

1.2 ml of DRM extract and 0.6 ml of total membrane extract reacted with, respectively, 1 ml or 0.5 ml of solution 0.5 M KOH in methanol and the resulting solution was stirred for 3 hours. The solution was neutralized with

3.5 Stress protocol and lipid extraction from larvae

few drops of sulfuric acid and was vacuum evaporated to dryness. 0.1 ml of hexane was added to the dried sample for GC-MS analysis. A Thermo-Finnigan Trace GC Ultra, equipped with a flame ionization detector and coupled to a Thermo-Finnigan Trace DSQ quadrupole mass spectrometer, was used to carry out the GC-MS analysis of FAMES derivatives. The chromatographic column used was a DB-WAX 30 m x 0.250 mm x 0.50 μ m. The temperature of the injector and detector were maintained constant at 250°C and 280°C, respectively. The flow of the carrier gas (He) was 1.0 ml/min. The source and the transfer line are maintained at 300°C. The detector gain is set at 1.0×10^5 (multiplier voltage: 1326 V). For every chromatographic run 1.0 μ l of sample solution was injected. The oven method starts with an initial temperature of 50 °C held for 1.0 min, followed by a linear ramp from 50 to 200 °C at 25 °C/min, from 200 to 230 °C at 3 °C/min. The final temperature of 230 °C was held for 19.0 min. The source filament and the electron multiplier were switched off during the initial 5 min to avoid the detection of the solvent front. Mass spectra were recorded with Chemical Ionization (CI) ion source. The mass range scanned was from m/z 50 to m/z 500 at 500 amu/s. Data were collected and processed with Xcalibur (version 1.4). Fatty acid methyl esters were identified by the comparison of their retention times for those of a reference solution run at identical GC conditions and by matching of the MS spectra with the MS-library implemented in the GC apparatus.

3.5 Stress protocol and lipid extraction from larvae

Specimens of *Pseudodiamesa branickii* and *Diamesa cinerella* at 4th larval stage were collected in the Noce Bianco stream (Trentino) in March 2009 and July 2009 respectively (average T= 4°C), and stocked in the laboratory facilities at 4°C for 1-4 days without feeding before experimental procedures. Animals (three replicates, 5 specimens for replicates or 1 replicate, 50 larvae) were stressed at decreasing temperature (2, 0, -1, -2, -3 and -4°C) for 30

Material and methods

minutes, with a decreasing temperature ratio of $-0.1^{\circ}\text{C}/2$ min. Animal survival was checked. Survival curves have been performed on larvae exposed to different temperatures. Animals were frozen at -80°C for further experimental procedures. The expression levels of all genes has been analyzed in stressed and control larvae via quantitative real-time RT-PCR. All these ecological and biochemical experiments have been carried out in the laboratories of the research group of Dr.ssa Lencioni (MTSN, Museo Tridentino di Scienze Naturali) and in the research group of Prof. Jousson (CIBIO, Centre for Integrative Biology, UNITN). For the lipids extraction from larvae we have adopted a two-steps procedure. In the first step, in according to literature [39], 2 ml of distilled water and 1 ml of chloroform were added to the larvae and hand-vortexed. The resultant two-phase mixture was allowed to sit for 30min and then vacuum-filtered through a glass filter; the filter was washed with 1 ml chloroform/methanol/water (2:1:0.8). After filtration the two-phase mixture was separated into an aqueous phase containing polar metabolites (sugars, polyols, amino acids) and an organic phase containing medium-low polar metabolites (lipids). The larvae, after this first extraction, were recovered from the glass filter and reextracted following Folch method [48]: 2 ml of chloroform and 1 ml of methanol were added, the mixture was sonicated for 10min, allowed to sit for 90min, sonicated for 10min and finally vacuum-filtered through a glass filter. The resulting solution, after a comparison with the previous organic phase by a TLC, was added to the previous one.

3.6 LC-MS Measurements

Lipid composition analysis: LC/ESI-MS analysis of the mixture of lipids was performed on a Hewlett-Packard Model 1100 Series liquid chromatograph coupled both to a PDAD (Photo Diode-Array Detector), Agilent 1100 Series, and to a Bruker Esquire-LC quadrupole ion-trap mass spectrometer equipped with atmospheric pressure ESI (electrospray ionization mass spec-

trometry) interface. Chromatography: C18 column (Phenomenex Kinetex 2.6u 100A); two eluents: A is $CH_3OH : H_2O + CH_3COONH_4 \ 28mM \ 7 : 3$ and B is $CH_3OH + CH_3COONH_4 \ 12mM$ with a gradient A/B starting from 30/70 to 0/100 with a flow 1ml/min. MS parameters: positive- and negative-ion mode ESI; dry gas 6 l/min, heated to 300oC. Further parameters during LC/MS analyses were: trap drive 54, skim 1 set at -43.2 V in negative mode and trap drive 44, skim 1 set at 43.2 V in positive mode. PC and SM lipids were identified in positive-ion mode extracting a chromatogram by the marker ion at m/z 184 and, then, searching the specific species by the molecular ion; the area of $[M + H]^+$ and $[M + Na]^+$ ions were integrated to obtain the percentage composition inside PC or SM class. PC species have been confirmed by negative-ion mode spectra identifying the corresponding $[M - 15]^-$ ion. SM species have been confirmed by negative-ion mode spectra identifying the corresponding $[M - H]^-$ ion. PE lipids were identified by the abundant ion $[M + H - 141]^+$ in positive-mode and its area was integrated to obtain the percentage composition inside PE class. PE species have been confirmed by negative-ion mode spectra identifying the corresponding $[M - H]^-$ ion. From negative-ion mode spectra information on fatty acyl chains of PE species have been obtained. For PC the same informations haven't been obtained because of the low intensity of the signals due to lower degree of ionization and fragmentation of PC in negative mode.

3.7 NMR Measurements

NMR analysis was performed with a Bruker Avance spectrometer operating at 400 MHz. We have used different conditions to perform different measurements on various sample.

DRM: 1H spectra were obtained in CD_3OD at 25 °C with the sequence zgpr to saturate water signal, and the calibration of the frequency-scale has done on proton-residual chemical shift of methanol (3.31 ppm). ^{31}P spectra were obtained in a solution of sodium cholate in D_2O 0.9 M at 25 °C; we have cal-

Material and methods

ibrated the spectra on external signal of H_3PO_4 in D_2O .

Chironomids larvae: 1H and ^{31}P spectra were obtained in a mixture $CDCl_3$: CD_3OD 2 : 1 at 25 °C. The calibration of the frequency-scale of proton spectra has done with proton-residual chemical shift of methanol (3.31 ppm); instead, the signal of PC has been chosen for the calibration of phosphorus spectra at -0.8 ppm [49]. 2D spectra (COSY, HSQC, HMBC) were obtained with standard Bruker pulse sequences at 25 °C in the previous conditions.

Chapter 4

Results and discussion

4.1 Standard mixture of lipids

Each phospholipid class has been tested by 1H NMR obtaining a list of characteristic signals for each class useful to recognize and assign them in the 1H NMR complex mixture spectrum. In the table 4.1 the peculiar peaks of the various classes are reported.

For phospholipids analysis, ^{31}P NMR is preferred to 1H NMR techniques since the signals are better resolved and do not overlap with signals from neutral lipids usually present in the extracts. However, in order to minimize the factors which heavily affect the true resolution of the acquired ^{31}P NMR spectrum of any PL mixtures, several factors have to be taken into account. First of all, electrostatic complexes with cations or anions must not occur or, if they do, the rate of exchange of the participating groups must be rapid with respect to the NMR time scale so that the phosphorus nucleus only senses an average electrostatic field. Furthermore, one must be well aware that the fatty acid side chains, which in a preparation from natural sources will be numerous and diverse, contribute little to the chemical shielding of the constituent phosphorus atoms. Last but not least, the contribution to the line width of chemical-shift anisotropy must be as low as possible [50]. The first problem is arising because in commonly used solvents, like $CDCl_3$

Results and discussion

δ (ppm)	PL class	Assignment
5.7	SM	olefinic proton of sphingosine base
5.45	SM	olefinic proton of sphingosine base
5.35	All classes	olefinic protons of fatty acid chains
5.18	alkyl-acyl PL	CH sn-2 glycerol
4.28	PC and SM	$PO - \bar{C}H_2 - CH_2 - N(Me)_3$
4.1	PE	$PO - \bar{C}H_2 - CH_2 - NH_3$
3.64	PC and SM	$PO - CH_2 - \bar{C}H_2 - N(Me)_3$
3.22	PC and SM	$CH_2 - N(\bar{C}H_3)_3$
3.18	PE	$\bar{C}H_2 - NH_3$
2.80	all PL	bis-allylic protons in PUFA chains
0.97	all PL	terminal methyls in omega-3 PUFA chains
0.90	all PL	terminal methyls in non omega-3 chains

Table 4.1: Peculiar peaks of 1H NMR spectrum in CD_3OD of phospholipids; the bar indicates the proton to which the signal is assigned

o CD_3OD , phospholipids create some aggregates whose tumbling motion is not so fast to obtain sharp linewidths (about 1 Hz). The variation of ^{31}P chemical shift is related to pH and ion concentration because these two factors modify polar heads of phospholipids by acid-base equilibrium [51] or electrostatic interactions. This problem has been tackled by many research groups with various solutions, looking for the best solvent system for NMR experiments [52]. In our work, in order to optimize the system, several solvent systems have been experimented: $CDCl_3$, $Et_3N/CD_3OD/Na_2EDTA$ (0.2 M in D_2O) 8/1/1 and $CDCl_3/CH_3OH/K_2EDTA$ (0.2 M) 8/4/1. In figure 4.1 and 4.2 some examples of ^{31}P NMR spectra of standard mixture of PL in these systems are shown.

EDTA is added to sequester metal ions from the solution avoiding the interaction of these ions with the head group of phospholipids. These spectra strongly underline problems related to signal's line broadening, the effect being so important to hinder the attribution of all the PL signals. This prob-

4.1 Standard mixture of lipids

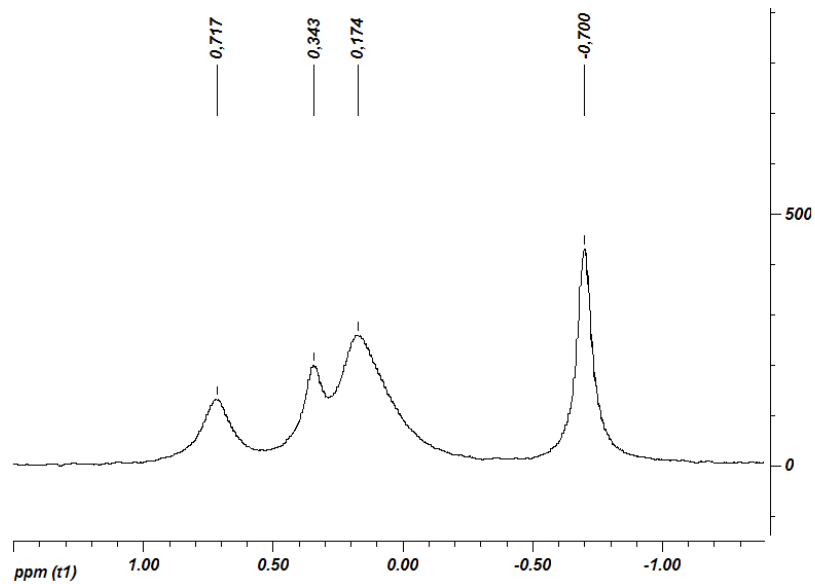


Figure 4.1: ^{31}P NMR spectrum of mixture 1 in CDCl_3

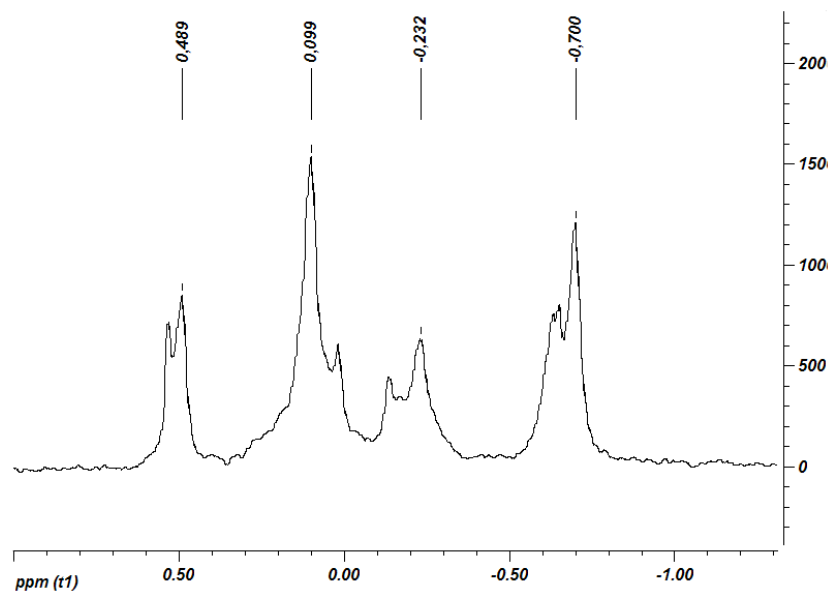


Figure 4.2: ^{31}P NMR spectrum of mixture 1 in $\text{Et}_3\text{N}/\text{CD}_3\text{OD}/\text{Na}_2\text{EDTA}$ (0.2 M in D_2O) 8/1/1

Results and discussion

lem is evident in the spectrum recorded in $CDCl_3$, where SM and PS have the same chemical shift and their signals overlap to those of PE and PI signal. Concerns due to the heterogeneous character of some solvent systems are also arising after looking at the corresponding ^{31}P NMR spectra. To overcome these problems another system was tested using a detergent. The optimal detergent should form small micelles with a fast tumbling motion [51]; sodium cholate fulfills these requirements because it forms small micelles with an aggregation number equal to four [53].

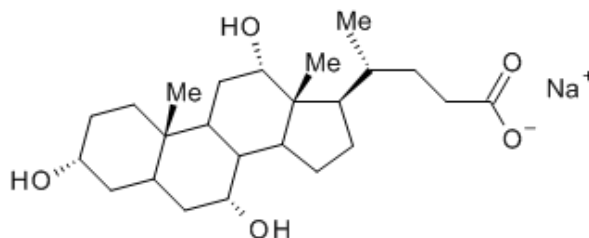


Figure 4.3: Molecular structure of sodium cholate

Although using sodium cholate PL class attribution is a straightforward (Figure 4.4), the complete resolution between SM and PE heads is not achieved.

Although solution-state NMR of cell extracts is considered a standard way of identifying tissue lipids providing useful information on their metabolic changes, there are some major drawbacks. In fact, the extraction processes are laborious, secondly there are risk of degradation and artefact generation, and finally only soluble components can be studied - not those associated with membranes cannot. A possible alternative to identify metabolites is to carry out analysis on whole tissue/cell samples by solid-state NMR technique with high resolution Magical Angle Spinning (HRMAS). By spinning a small intact tissue sample at the well known 'magic angle' of 54.7° in principle, we could obtain spectra of resolution comparable to liquid-state NMR of extracts. In fact, spinning at the magic angle counteracts the line broadening effects resulting from the restricted motion of the molecules in

4.1 Standard mixture of lipids

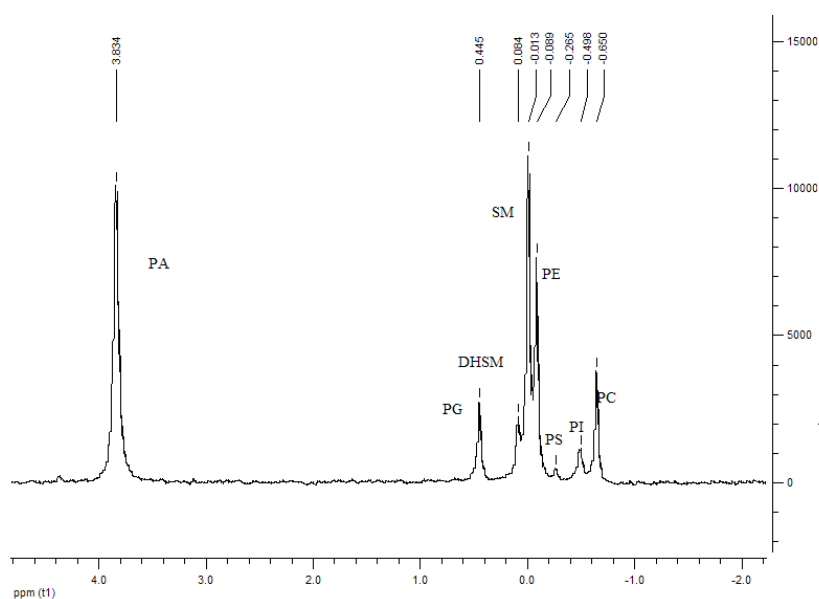


Figure 4.4: ^{31}P NMR spectrum of mixture **2** in solution of sodium cholate in D_2O 0.9 M

the solid state. More specifically, there is no dipolar coupling and chemical shift anisotropy when a sample is spun at the magic angle.

Looking for avoiding chemical workup of the biological samples, we did some experiments on solid state NMR trying to obtain a resolution similar to high-resolution NMR. However, results were far behind the expectations based on recent literature reports (Figure 4.5); suffice to say that all the signals attributable to the main PL classes were buried under a single broad resonance. The two signals at -12 ppm are due to phosphorus nuclei of ATP.

This spectrum has shown that solid-state NMR does not provide enough resolution to acquire significant information about the composition of the membrane in ex-vivo sample. For this reason high-resolution NMR on liquid extracts has been chosen as the technique to obtain a reliable quantification of phospholipids in our biological samples.

Results and discussion

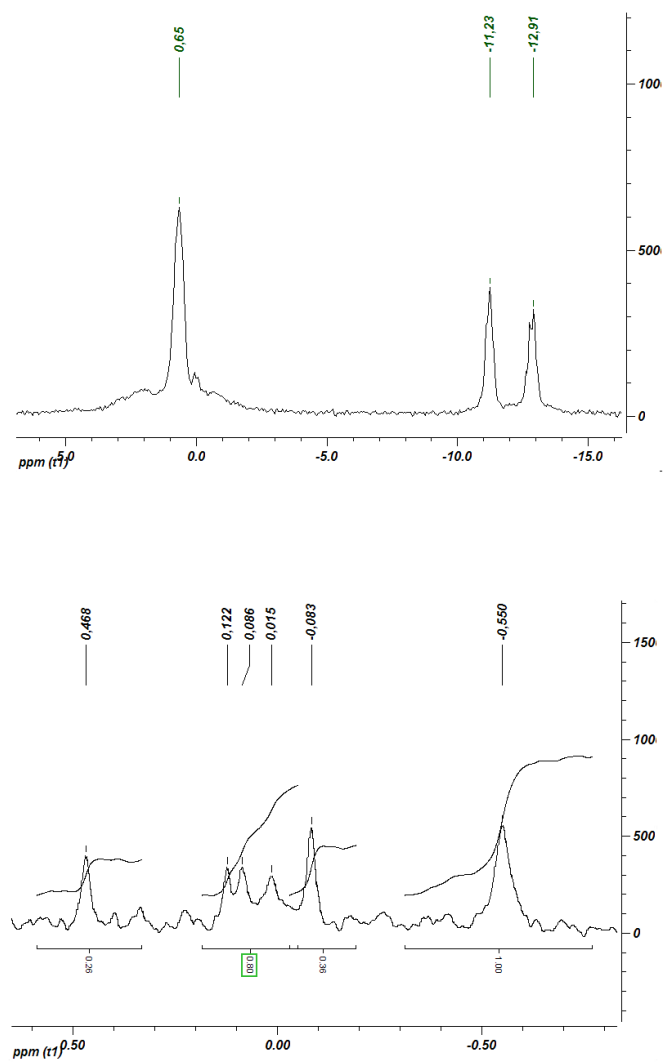


Figure 4.5: top: SS ^{31}P NMR spectrum of LNCaP cells at 298 K and a MAS frequency of 2 kHz; bottom: high resolution ^{31}P NMR spectrum of lipid extract from LNCaP cells at 298 K in sodium cholate solution 0.9 M in D_2O

4.2 Lipid profile of PSMA-anchoring rafts

The extracted lipid components were analyzed by different analytical techniques. A qualitative screening was made by thin layer chromatography followed by an extended NMR analysis of the sample. In particular, 1H and ^{31}P NMR spectra allowed to detect and quantify cholesterol and the relative contribution of all the lipids belonging to a given PL class to the overall PL composition. From 1H spectra (see figure 4.6 and 4.7) the molar ratio between cholesterol and choline lipids (PC+SM) has been evaluated by integration of the singlet at 3.22 ppm for choline lipids (methyl groups of tetramethylammonium group) and the singlet at 0.72 ppm for cholesterol (methyl group in C18 position). This ratio is 0.52 in whole cell membranes and to 0.84 in Lubrol DRMs, with a 60% increase.

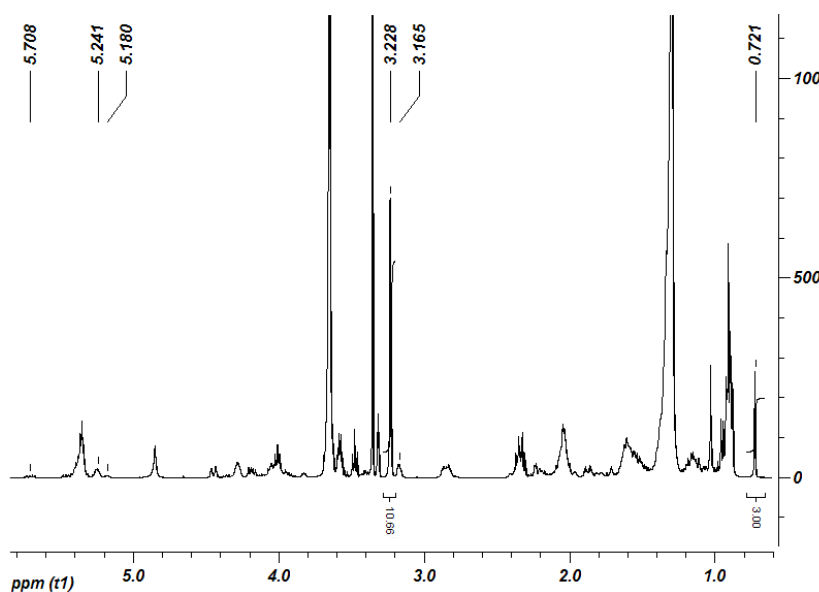


Figure 4.6: 1H spectrum of DRM extract in CD_3OD

From ^{31}P spectra (see figure 4.8 and 4.9) we have resolved the composition of various phospholipids.

In the ^{31}P spectra there is only partial resolution between the signals of SM and PE but the deconvolution of the spectra by lorentzian functions (see

Results and discussion

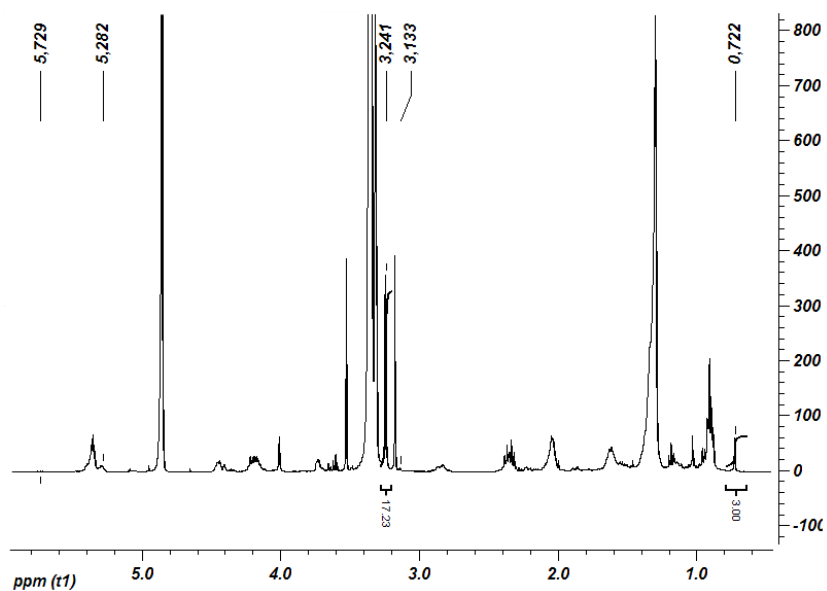


Figure 4.7: ^1H spectrum of whole cell membrane extract in CD_3OD

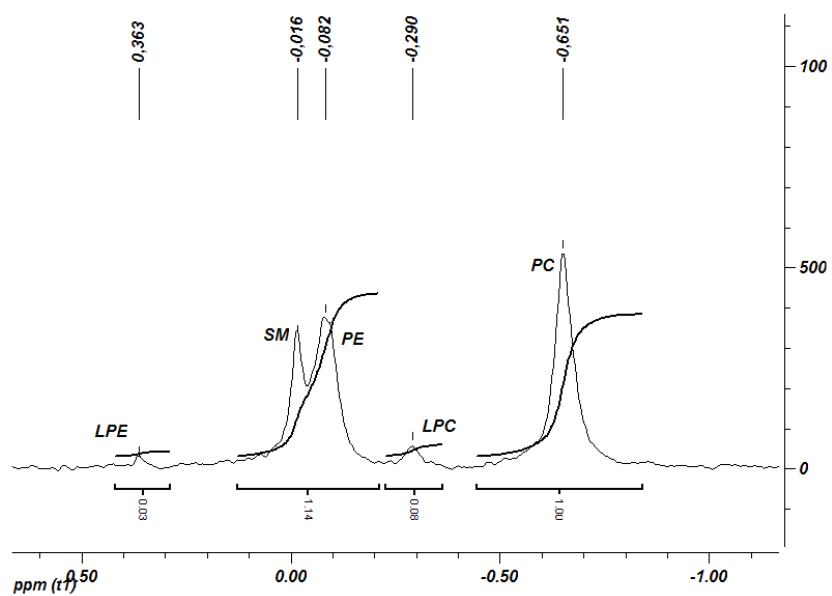


Figure 4.8: ^{31}P spectrum of DRM extract in sodium cholate solution 0.9 M in D_2O

4.2 Lipid profile of PSMA-anchoring rafts

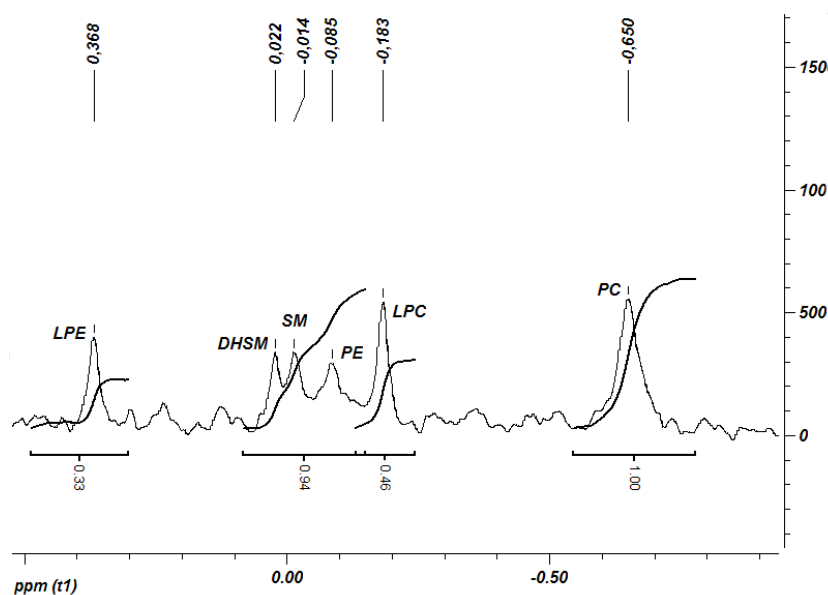


Figure 4.9: ^{31}P spectrum of whole cell membrane extract in sodium cholate solution 0.9 M in D_2O

figure 4.10 and 4.11) allowed us to obtain the reliable values for the SM and PE molar ratios.

From ^{31}P spectra and their deconvolution the total composition of PL in whole cell membrane and DRM has been obtained and is graphically shown in figure 4.12.

On the other hand, Electrospray Ionization (ESI-MS) measurements carried out on the same sample allowed us to establish some structural details such as the length and the degree of unsaturation of their acyl chains. The performed mass spectrometric analysis only allowed the determination of the total number of carbon atoms and double bonds in the FA moiety for lipid classes containing two FA esterified to the glycerol-backbone (PC, PE, PG, PI, PS). For example a PC 34:1 may represent different combinations of FA such as 18:0/16:1, 16:0/18:1, etc. Moreover, the assignment to a bond type (acyl or ether) is based on the assumption that FA with odd-numbered carbon atoms are not present at all or, at least, represent a negligible fraction of the overall lipid amount. Therefore, when structural information is

Results and discussion

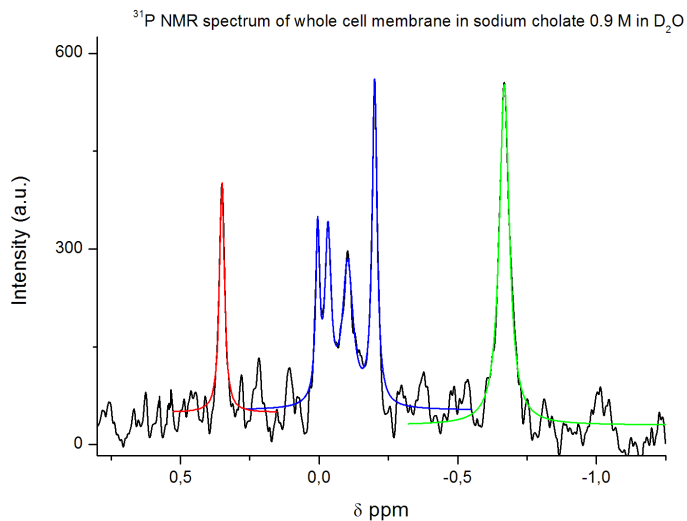


Figure 4.10: ³¹P spectrum of whole cell membrane extract in sodium cholate solution 0.9 M in D₂O with deconvolution of the signals by lorentzian functions

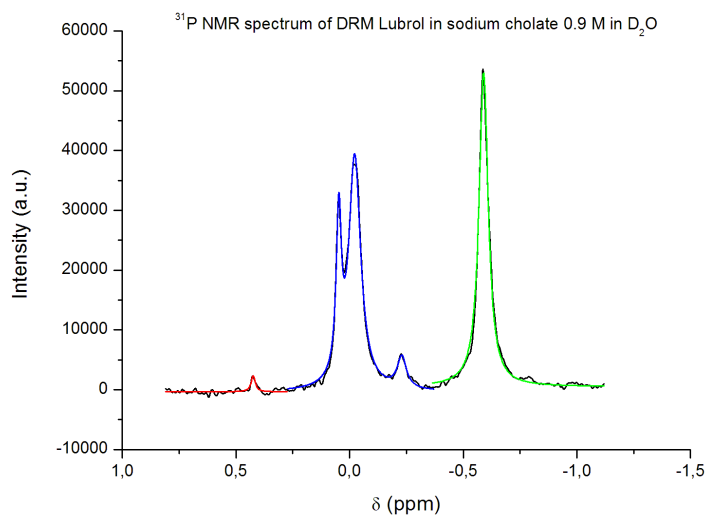


Figure 4.11: ³¹P spectrum of DRM extract in sodium cholate solution 0.9 M in D₂O with deconvolution of the signals by lorentzian functions

4.2 Lipid profile of PSMA-anchoring rafts

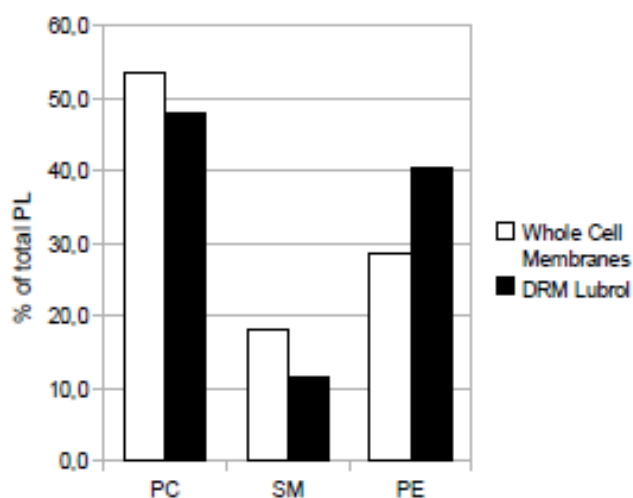


Figure 4.12: Composition of phospholipids classes in whole cell membrane and DRM obtained by ^{31}P spectra and their deconvolution

required, tandem mass spectrometry (MS/MS) was employed. In this procedure, the precursor ion undergoes further fragmentation either by collision-induced dissociation (CID) or spontaneous in-source dissociation. In the following figures are shown the LC chromatogram of DRM and the distribution of all PC, PE and SM identified by MS analysis.

For PE, from negative-ion mode ESI, information about the single fatty acid chain of the lipids has been obtained (see table 4.2).

Furthermore, GC-MS analysis of FAME (fatty acid methyl ester) extracted from whole cell membrane and DRM samples has been afforded (see figure 4.17).

The comparison between LC-MS and GC-MS data did not show to be possible; GC measurements lead to reliable quantitative data because the integration is done on peaks detected by a Flame Ionization Detector (FID) whereas, ESI measurements do not usually lead to quantitative data because the signal intensity depends on the degree of ionization, which, in turn, depends on the acyl length, unsaturation of fatty acid chain and lipid concentration [10]. This difference is well notable if we analyze the arachi-

Results and discussion

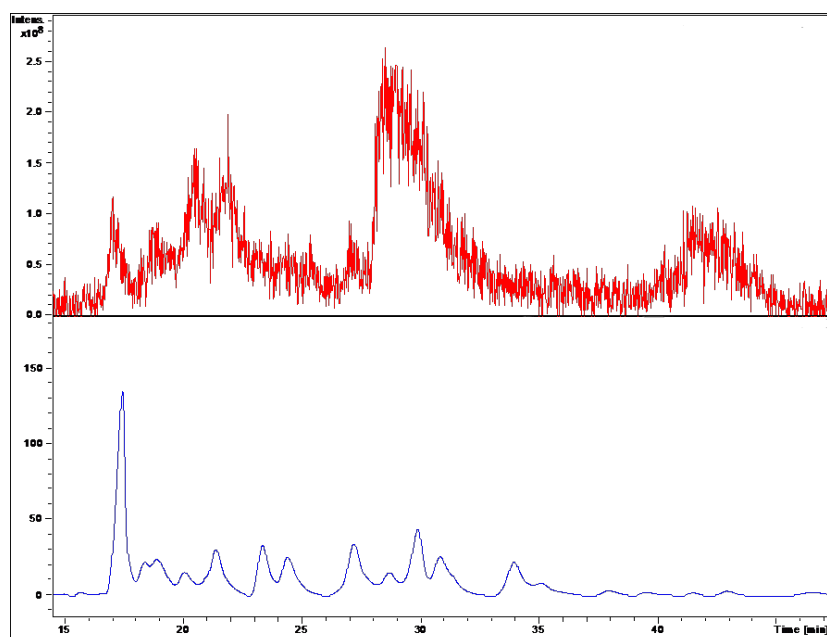


Figure 4.13: LC-MS chromatogram of a DRM extract. Top: chromatogram based on total ion current. Bottom: chromatogram based on UV absorption at 215 nm

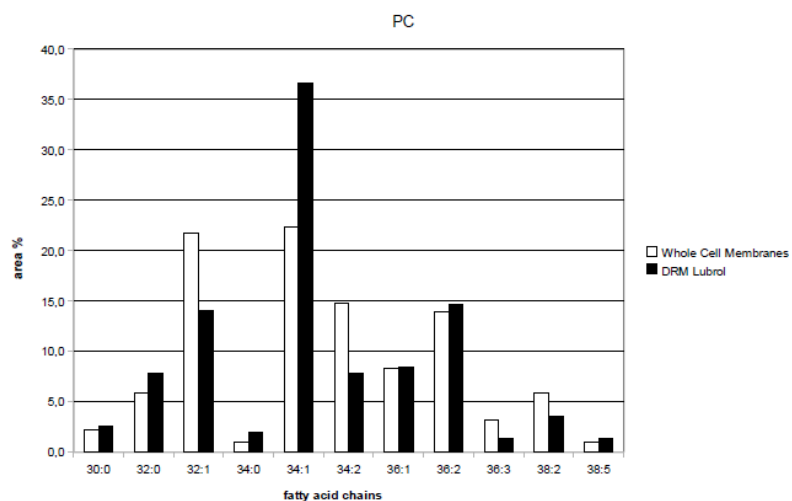


Figure 4.14: Distribution of PC in whole cell membrane and DRM as obtained by LC-MS experiment

4.2 Lipid profile of PSMA-anchoring rafts

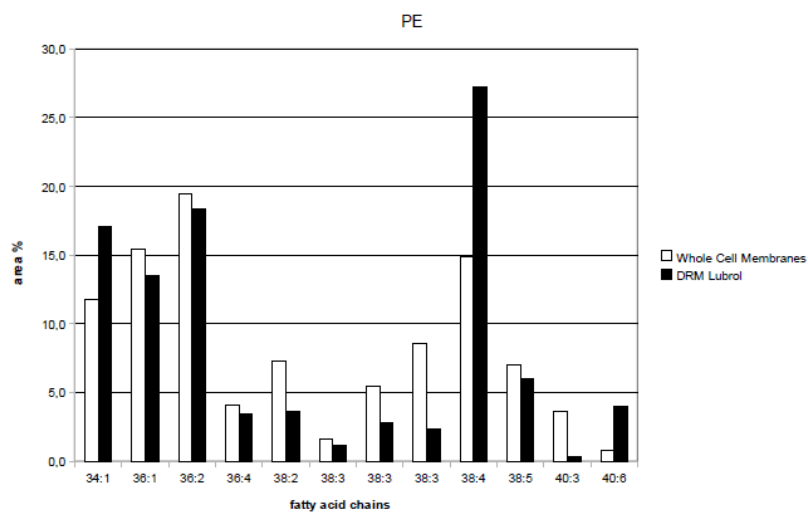


Figure 4.15: Distribution of PE in whole cell membrane and DRM as obtained by LC-MS experiment

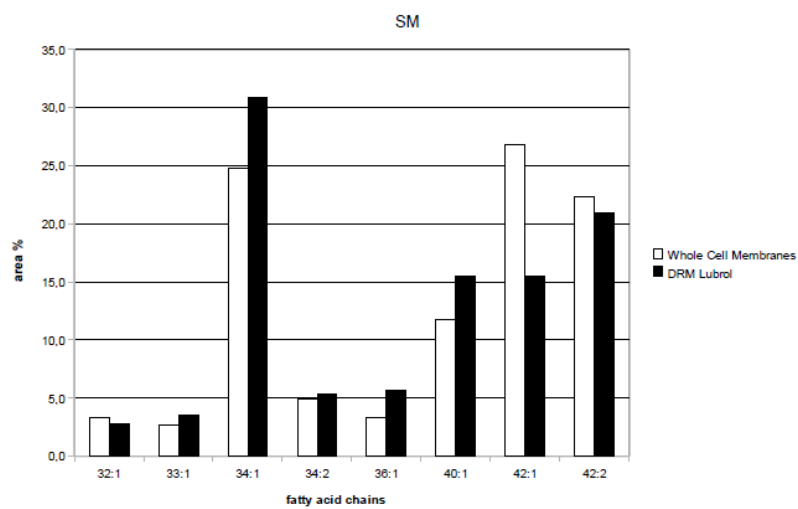


Figure 4.16: Distribution of SM in whole cell membrane and DRM as obtained by LC-MS experiment

Results and discussion

PE lipid	Chain 1	Chain 2
34:1	18:1	16:0
36:1	18:0	18:1
36:2	18:1	18:1
36:4	20:4	16:0
38:2	Unknown	Unknown
38:3	20:3	18:0
38:3	Unknown	Unknown
38:3	Unknown	Unknown
38:4	20:4	18:0
38:5	20:4	18:1
40:3	Unknown	Unknown
40:6	22:6	18:0

Table 4.2: Fatty acid chains of PE lipids from negative-ion mode ESI

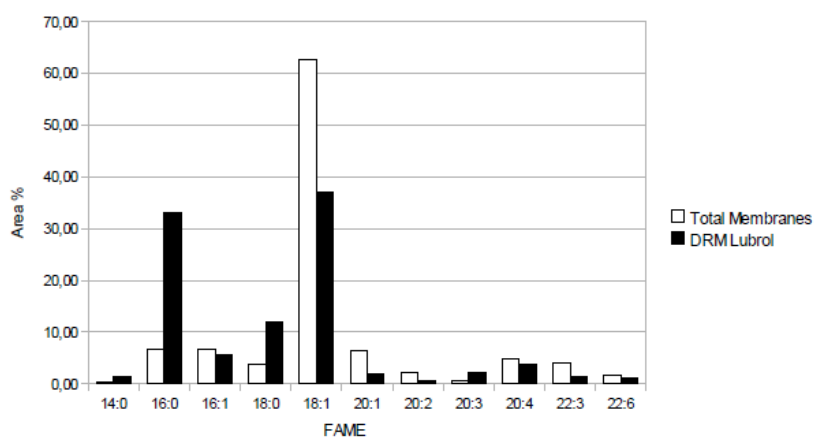


Figure 4.17: Distribution of FAME in whole cell membrane and DRM

4.2 Lipid profile of PSMA-anchoring rafts

donic chain (20:4). On the basis of LC-MS data this chain is one of the two acyl chains of 38:4 PE, one of the major PE presents in both the extracts; nevertheless, analyzing GC data, arachidonic methyl ester is only 5% of the total fatty acid methyl esters. This difference arises because arachidonic acid has a polyunsaturated chain and PUFAs in ESI are overestimated. LC-MS data show the principal phospholipids of whole cell membrane and DRM; in all the classes (PC, SM and PE) there is a clear predominance of lipids with saturated or monounsaturated fatty acid chains, except PE where there are some polyunsaturated chains like 20:3, 20:4 and 22:6. This tendency of PE towards more unsaturated chains is confirmed by the value of the mean unsaturation index, calculated from LC data, of PE with respect to PC and SM (2,7 for PE versus 1,2 for PC and SM). GC data show that in DRM there is a noticeable increase of palmitic chain whereas there is a clear decrease of oleic acid. This outcome is in agreement with the model of DRM, where a chain shorter and saturated leads to a more rigid and more resistant membrane structure and is partitioned preferentially in the liquid-ordered phase. The same observation could be done on LC data of sphingomyelins where in DRM the palmitic chain is the main chain with a marked decrease of tetracosanoic chain with regard to the whole cell membrane. LC-MS data speak for the presence of alkyl-acyl PC, where the fatty acid chain in sn-1 position is bound through an ether bond instead of an ester. The chemical shift of the proton at the secondary glycerol position in 1-alkyl-2-acyl lipids is, in fact, more shielded (5.18 ppm) in comparison to that of 1,2-diacyl lipids (5.25 ppm) (figure 4.6). Indeed, the correlation observed in HSQC $^{13}\text{C} - ^1\text{H}$ spectrum confirms that the signal at 5.18 ppm is the proton attached to carbon atom in position 2 of the glycerol (signal at 72 ppm) (see the insert in figure 4.18).

These data are not in agreement with the usual reports on DRM composition, i.e. that a peculiar feature of DRM is the high percentage of sphingomyelins in comparison to the other phospholipids. This concern arises because, in our investigations Lubrol was chosen as detergent whereas in

Results and discussion

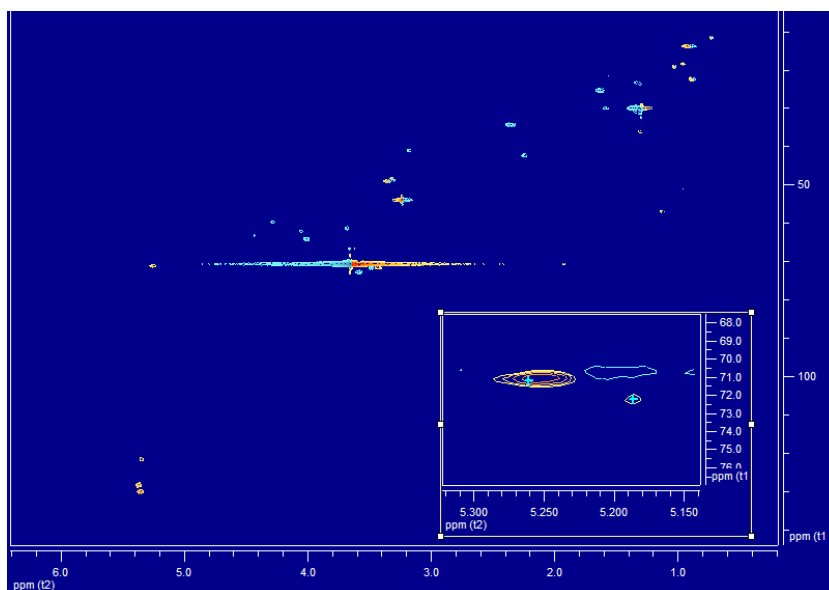


Figure 4.18: HSQC $^{13}\text{C} - ^1\text{H}$ spectrum of DRM extract in CD_3OD

almost all literature reports Triton X100 (more aggressive) is used. Lubrol has been chosen as detergent because PSMA has shown a differential association with DRM corresponding to isolation with Lubrol but not TX-100. Lubrol has been reported being to be a mild detergent leading to the formation of DRMs without denaturing membrane proteins. The distinctive feature of Lubrol is to favor the formation of DRM with a composition similar to the whole cell membrane without promoting the enrichment in sphingolipids and cholesterol as Triton does [17]. NMR data confirm this assumption because PC and PE are the two principal classes in both cases (DRM and whole cell membranes) although the amount of PE increases around 40% in DRMs demonstrating a tendency of Lubrol to provide DRM with an higher PE concentration. The PLs molar ratio of DRM in this work is in agreement with a previous work on similar samples [25], confirming the validity of our results. It is known from literature that cholesterol interacts with phospholipids and the strength of this interaction depends on the headgroup (SM>PC>PE) and on the degree of saturation of the acyl lipid chain (saturated > monounsaturated » polyunsaturated); the strongest in-

4.3 Cold resistance in Chironomid larvae

teraction occurs with sphingolipids because they have, usually, saturated chain and can form hydrogen bonding between the NH group of sphingosine base and the hydroxyl group of cholesterol. It has been shown [54] [55] the inability of cholesterol to intercalate in model membranes composed exclusively of PUFA (22:6/22:6 PC or 22:6/22:6 PE) because close proximity to the sterol of polyunsaturated chains is hindered by their high degree of disorder; however it has been demonstrated that in model membrane, composed by lipids like 18:0/22:6 PC, the near approach and the intercalation of cholesterol is facilitated by the configuration adopted by the upper portion of the saturated chain. Our data confirm the importance of cholesterol to trigger rafts formation because in DRM there is an increase of cholesterol around to 60%. The preference of rafts for saturated or monounsaturated fatty acid chains is confirmed by our results, because GC data show that polyunsaturated chains (20:4, 22:3 and 22:6) represent only the 10% of the total fatty acid and the two most abundant FAMES are 16:0 and 18:1. Regarding the composition, the high percentage of PE is not in contrast with literature because it has been demonstrated the less aggressive properties of Lubrol compared to Triton X-100 and its tendency to form DRMs with a composition similar to whole cell membrane. Furthermore our results demonstrate that the main driving force to the rafts formation is the acyl chain packing and the interaction of cholesterol with saturated or monounsaturated fatty acid chains other than lipid headgroup. This study supports the model that lipid raft stability is conferred by acyl chain structure and its interaction with cholesterol.

4.3 Cold resistance in Chironomid larvae

In this chapter we report the results obtained in the studies of larvae of two species chosen as target samples to observe the influence of environmental changes on alpine ecosystems. The two species investigated are *Pseudodiamesa branickii* and *Diamesa cinerella*. The main membrane lipid

Results and discussion

components (fatty acids, glycerolipids and phospholipids) have been characterized with mass spectrometry and NMR techniques. Particular attention has been paid to phospholipids, membrane constituents that are expected to change in response to freezing, both in the acyl chains and/or in their polar heads. A preliminary analysis of cryoprotectants such as polyols and sugars involved in cold hardness has been also carried out by different spectroscopic techniques. Overall, the experimental approach outlined has been led to a better understanding of the abiotic factors that represent major selective constraints to various aquatic taxa.

4.3.1 *Diamesa cinerella*

A qualitative screening made by thin layer chromatography (TLC) has shown that triglycerides and phospholipids are the main components of the total lipid fraction in these larvae. 1H NMR data (figure 4.19) have also shown a very low quantity of cholesterol (< 1%, signal at 0.68 ppm).

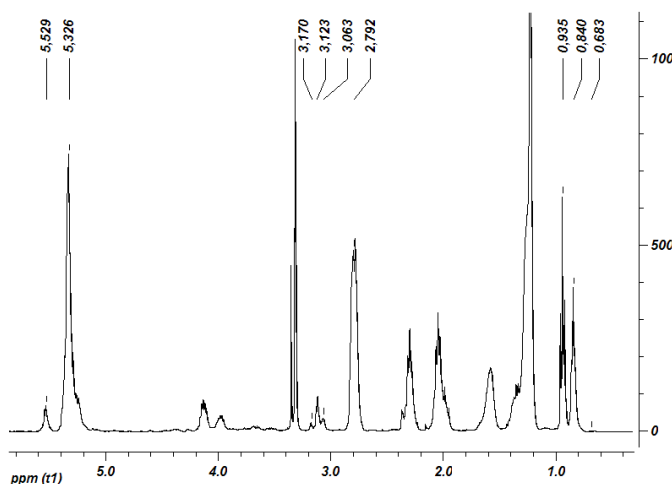


Figure 4.19: 1H NMR spectrum of raw organic extract of *Diamesa cinerella* in $CDCl_3 : CD_3OD$ 2 : 1

From 1H NMR spectrum it's clear the presence of a significant amount of PUFA chains, as established by the relative high integral ratio of the peak

4.3 Cold resistance in Chironomid larvae

at 2.8 ppm (allylic methylene groups) and the presence of the characteristic signal of terminal methyl group of omega-3 chains at 0.94 ppm, very sharp by comparison with the signal at 0.85 ppm relative to the methyl groups of the omega-6 and/or saturated chains. It's common practice in lipids analysis to obtain from 1H NMR spectra the mean unsaturation degree of the sample analyzed simply with the weighted ratio of the integrals of the signal at 5.35 ppm (olefinic protons) and those of the methyls terminal of the fatty chains. Since proton NMR signals from TAGs and PLs are heavily overlapped in these regions, the relative contributions of PL classes have been established by ^{31}P NMR measurements. ^{31}P NMR spectrum has been recorded (see figure 4.20) to obtain the composition of the phospholipids classes presents in the total lipid fraction without interferences by triglycerides signals.

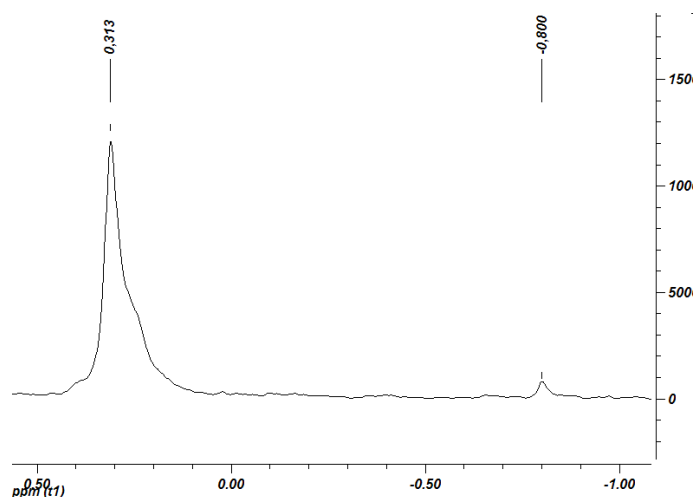


Figure 4.20: ^{31}P NMR spectrum of raw organic extract of *Diamesa cinerella* in $CDCl_3 : CD_3OD$ 2 : 1

This analysis shows that PL in *Diamesa cinerella* are essentially represented by PC and mainly PE, and that the predominant is PE. The percentage composition of these two classes is represented in figure 4.21.

This simple composition (only PC and PE) is in agreement with the data obtained on other similar insects [56]. The ratio between PE and PC does not change in larvae thermally adapted to +4 °C with respect those sub-

Results and discussion

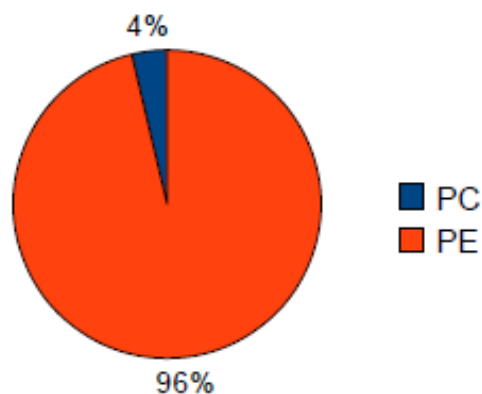


Figure 4.21: Percentage composition of *Diamesa cinerella* obtained by ^{31}P NMR data

jected to $-4\text{ }^{\circ}\text{C}$. To investigate more deeply the differences at these two temperatures, representing the vital range of these larvae, HPLC/ESI-MS experiments have been carried out (figure 4.22) allowing the identification of all the fatty chains bound to these two PL classes.

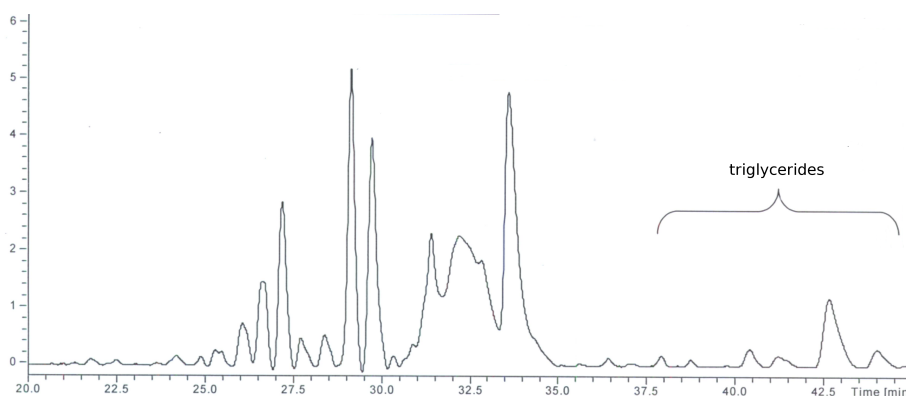


Figure 4.22: UV chromatogram LC of *Diamesa cinerella*

The fatty chains distribution of PE (figure 4.23) presents remarkable differences between the two temperatures. Although in both cases the main components in the lipid pattern are the chains 32:4, 34:5 and 36:5, in the

4.3 Cold resistance in Chironomid larvae

high temperature adaptation-system 32:4 is significantly more populated than in the low temperature adapted larvae. On the other hand the latter present a PL distribution richer in the chains 32:5 and 36:5.

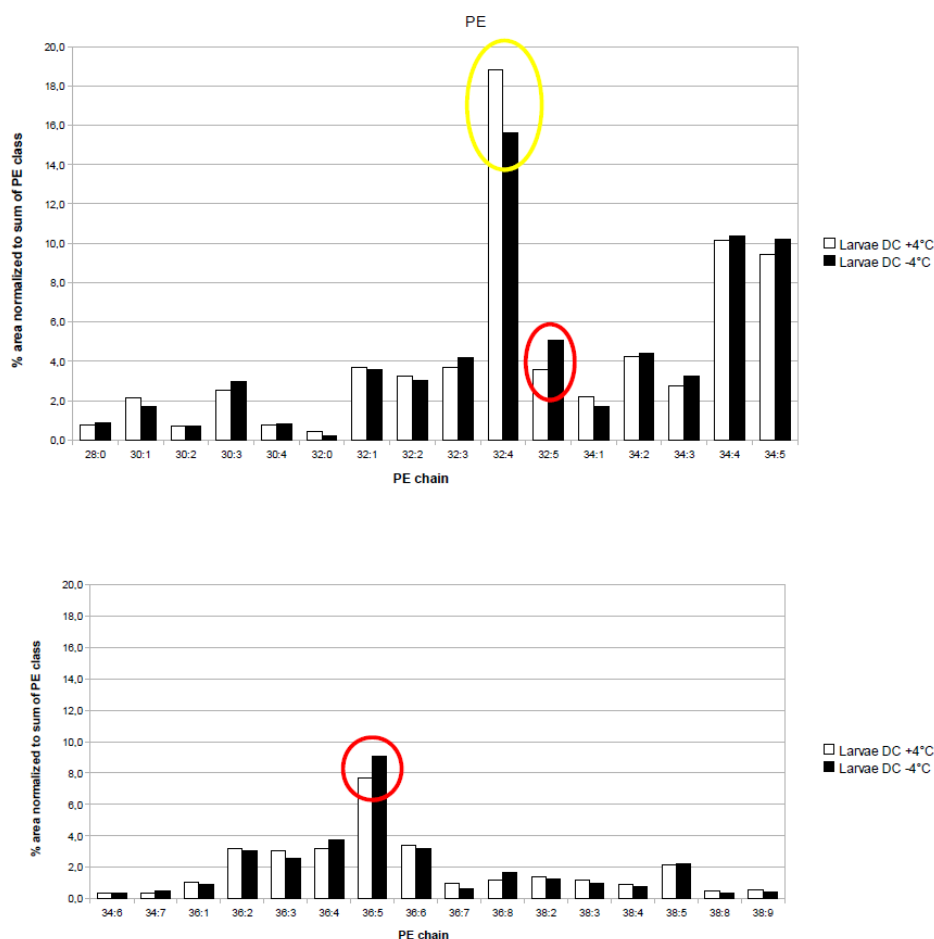


Figure 4.23: Distribution of PE in *Diamesa cinerella* at +4°C and -4°C as obtained by LC-MS experiment

For PE, from negative-ion mode ESI, it has been possible to obtain information about the single fatty acid chain of the lipids. In table 4.3 recognized chains are reported.

The data shown in table 4.3 confirm the high unsaturation degree of PE. When there is a pair of chain, one short and more saturated and the other

Results and discussion

PE lipid	Chain 1	Chain 2	PE lipid	Chain 1	Chain 2
28:0	Unknown	Unknown	34:6	Unknown	Unknown
30:1	14:0	16:1	34:7	18:4	16:3
30:2	Unknown	Unknown	36:1	18:0	18:1
30:3	14:0	16:3	36:2	18:0	18:2
30:4	Unknown	Unknown	36:2	18:1	18:1
30:4	Unknown	Unknown	36:3	18:0	18:3
32:0	Unknown	Unknown	36:3	18:1	18:2
32:1	14:0	18:1	36:4	18:0	18:4
32:2	14:0	18:2	36:5	16:0	20:5
32:3	14:0	18:3	36:5	18:1	18:4
32:3	16:0	16:3	36:6	14:0	22:6
32:4	14:0	18:4	36:6	Unknown	Unknown
32:5	14:0	18:5	36:6	18:2	18:4
34:1	16:0	18:1	36:7	Unknown	Unknown
34:2	16:0	18:2	36:8	18:4	18:4
34:2	Unknown	Unknown	38:2	20:0	18:2
34:3	18:0	16:3	38:3	20:0	18:3
34:3	16:0	18:3	38:3	Unknown	Unknown
34:4	16:0	18:4	38:4	20:0	18:4
34:4	Unknown	Unknown	38:5	18:0	20:5
34:5	Unknown	Unknown	38:8	Unknown	Unknown
34:5	14:0	20:5	38:9	Unknown	Unknown
34:5	Unknown	Unknown			

Table 4.3: Fatty acid chains of PE lipids from negative-ion mode ESI in *Diamesa cinerella*

4.3 Cold resistance in Chironomid larvae

longer and with an higher unsaturation degree, it's clear from literature that the more unsaturated chain preferred the sn2 position, because in this way it creates more disorder [57]. Observing the chains identified in PE it's possible noting some characteristic sequences of lipids with one chain fixed and varying the other, like the sequence based on the couple 14:0/18:x (x=1-5) or the couple 16:0/18:x (x=1-4). In the sequence based on 14:0/18:x, the last species is a particular lipid with a double bond in position $\Delta 3$, as shown in figure 4.24.

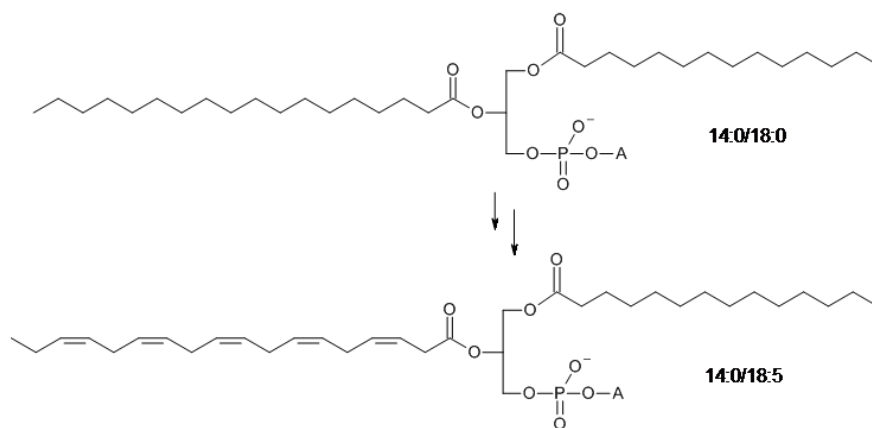


Figure 4.24: Sequence of PE with 32 C chains

This structure is confirmed by NMR data showing a specific signal at 5.53 ppm due to olefinic protons in $\Delta 3$ position [58] and its correlation with a signal at 3.12 ppm, due to methylene in $\Delta 2$ position, and with a peak at 2.80 ppm, due to bis-allylic methylene group (see figure 4.25).

This double bond position is unusual but, recently, in literature has been reported the presence of a phospholipid species containing a double bond in $\Delta 3$ position and they have identified the protein responsible of this synthesis, a $\Delta 3$ desaturase codified by fad4 gene [59]. From the ESI negative-ion data we could infer that one of the main solution adopted by these larvae to obtain lipids with an high mean unsaturation degree seems to be the insertion of a polyunsaturated chain omega3 like 20:5 or 22:6 (see figure 4.26).

Results and discussion

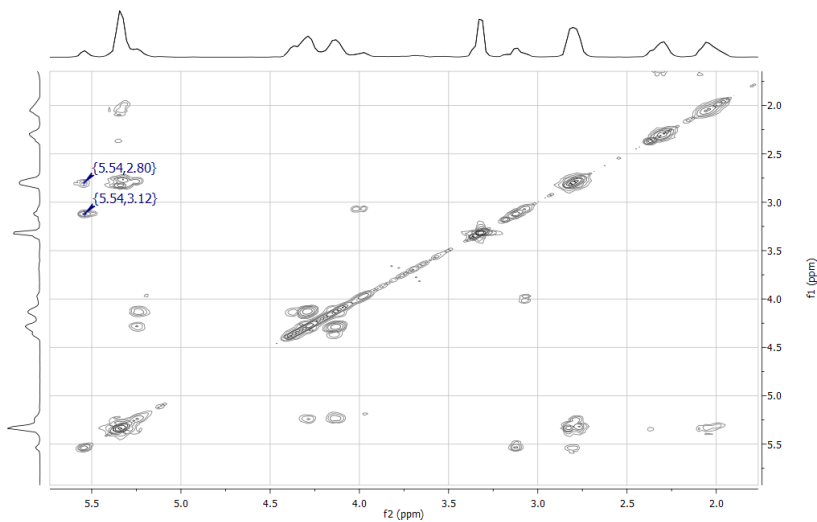


Figure 4.25: COSY of raw organic extract of *Diamesa cinerella* (+4 °C) in CDCl₃/CD₃OD 2:1

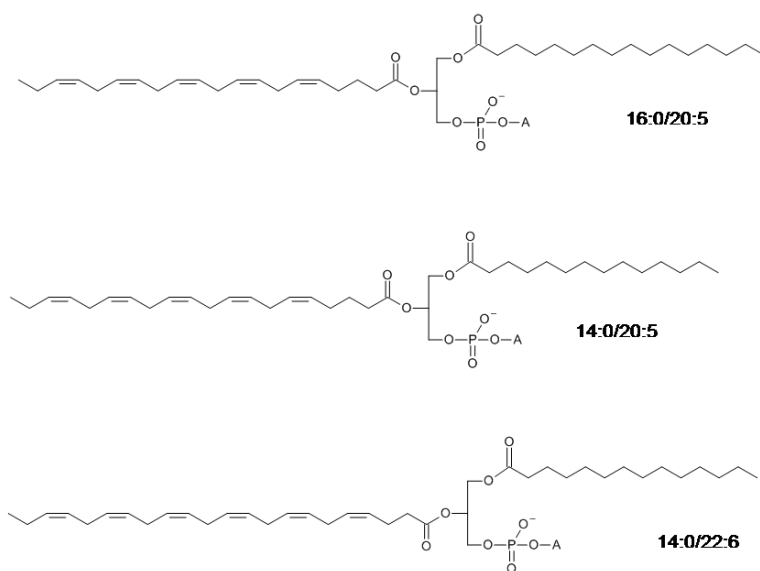


Figure 4.26: Principal PUFA found in organic extract of *Diamesa cinerella*

4.3 Cold resistance in Chironomid larvae

Another very interesting finding is the presence in the lipid profile of these larvae of one particular PE with a characteristic fragment at m/z 155 present in the ionization pattern of these species. This fragment from a PE lipid can be obtained by two molecules: a phosphopropanolamine or a phosphoethanolamine methyl ester. Whereas the last one is a rare molecule, the first is more common, especially in its analog form phosphopropylcholine. For this reason a structure of phosphopropanolamine has been proposed but there are not strictly NMR data confirming this hypothesis because signals are too little due to the low quantity of these species (ratio $PE_x/PE < 1\%$).

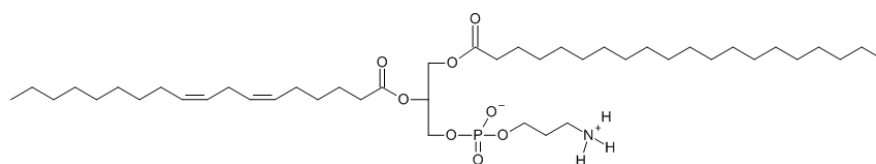


Figure 4.27: Structure of phosphopropanolamine

Summing up the previous descriptions, as shown in figure 4.28, there is a general trend about the distribution by number of carbon atoms of the two fatty acid chains over the all PE, allowing us to assert that the species with a lower number of carbon atoms (32) are more slightly prevalent at $+4^{\circ}\text{C}$ and at -4°C are little predominant species with an higher number of carbon atoms (34 and 36).

Comparing the PE mean unsaturation degree at the two temperatures, a little increase going down from $+4$ to -4 is observed and this aspect agree with the predict model, because more unsaturation of the chain means more disorder in the membrane and a resulting structure more flexible and resi-

Results and discussion

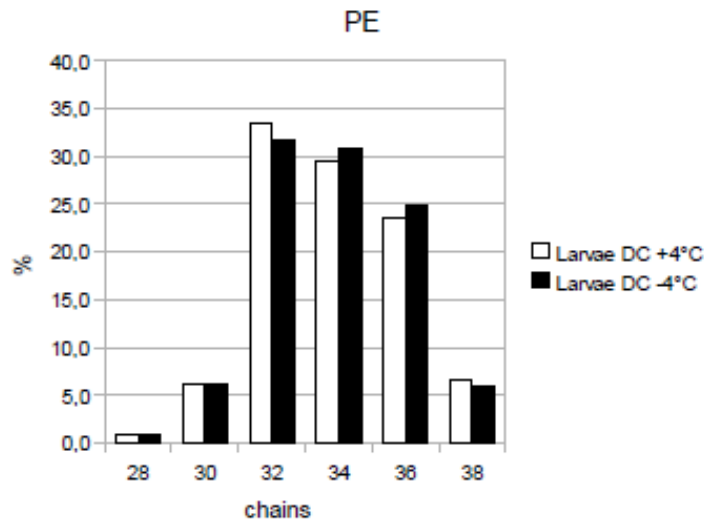


Figure 4.28: Distribution of PE divided by number of carbon atoms of the two fatty acid chains in *Diamesa cinerella*

stant to a lower temperature.

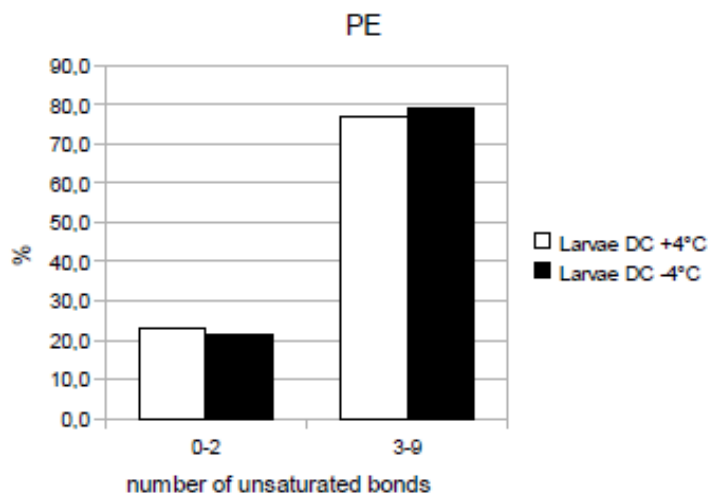


Figure 4.29: Distribution of PE divided by number of unsaturated bonds of the two fatty acid chains in *Diamesa cinerella*

As shown in the figure 4.30, in the distribution of PC there are some

4.3 Cold resistance in Chironomid larvae

remarkable differences between the two temperatures: at +4 °C there is a relevant dominance of the species 34:5 and 38:9 (yellow circles), at -4 °C the species predominant are 34:2 and 36:8 (red circles). Furthermore the main components in the lipid pattern are 32:4, 34:2, 34:4 and 36:5 PC.

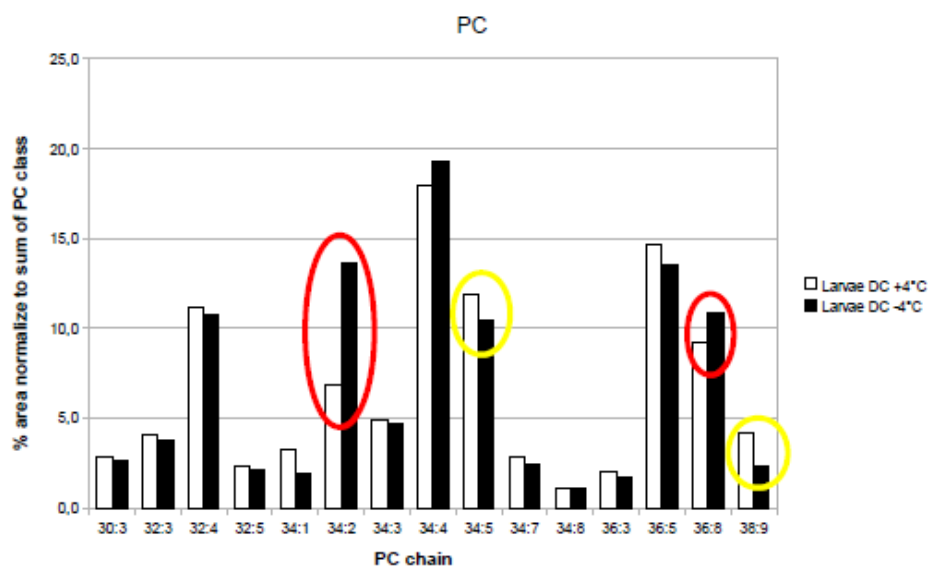


Figure 4.30: Distribution of PC in *Diamesa cinerella* at +4°C and -4°C as obtained by LC-MS experiment

Like to PE, the corresponding specie has been found, identified by the fragment 198 present in the ionization pattern of these species. Also for this specie a structure of phosphopropylcholine has been hypothesized but there are not reliable NMR data confirming this hypothesis.

For PC it has not been possible doing a sure assignment of the fatty acid chains because of the low intensity of signals. Summing up the previous descriptions, as we can see from figure 4.32, there is a significant increase of the lipids with 34 carbon atoms at -4°C whereas for the other chains there isn't a preponderance in one of the two cases.

For these extracts GC-MS experiments have not been carried out because of the low quantity of the two samples.

Results and discussion

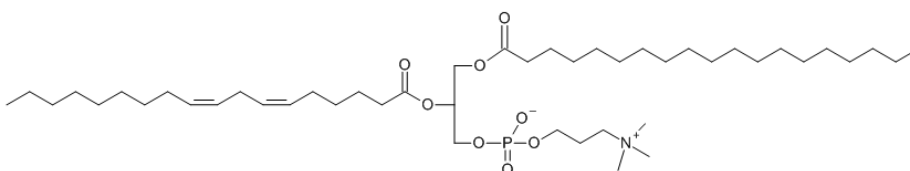


Figure 4.31: Structure of phosphopropylcholine

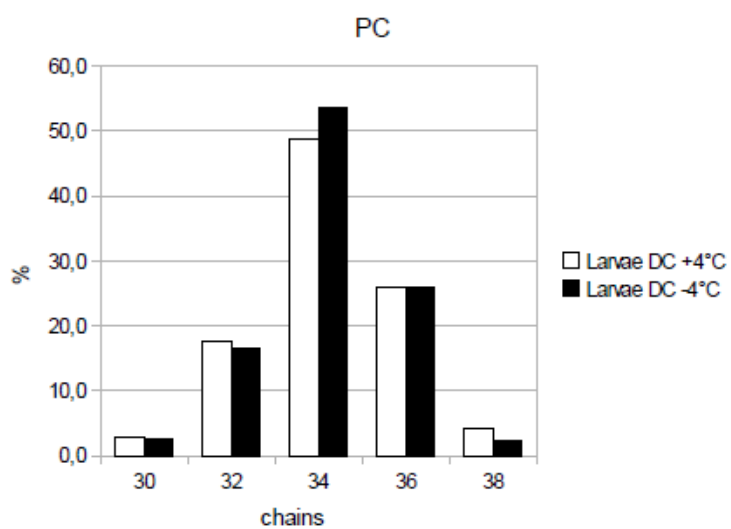


Figure 4.32: Distribution of PC divided by number of carbon atoms of the two fatty acid chains in *Diamesa cinerella*

4.3 Cold resistance in Chironomid larvae

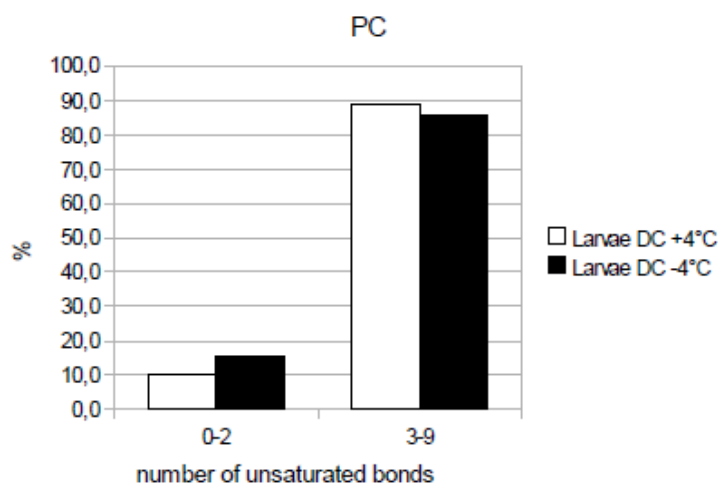


Figure 4.33: Distribution of PC divided by number of unsaturated bonds of the two fatty acid chains in *Diamesa cinerella*

The analysis of aqueous extracts has been carried out first by NMR; because the NMR spectrum is too crowded with signals and it has not been possible to make a sure assignment of the various peaks, HPLC/ESI-MS experiments in positive and negative ion mode have been accomplished to identify sugars and polyols presents in the samples and to observe if there are some significant trends with the temperature. Some sugars have been identified (glucose, sorbitol, sucrose, raffinose and lactose) but not trehalose, and the concentration of these molecules are similar without significant differences between the two samples at +4 and -4 °C.

4.3.2 *Pseudodiamesa branickii*

In *Pseudodiamesa branickii* we have found results similar to *Diamesa cinerella* (low quantity of cholesterol, significant amount of PUFA chains, impossibility to separate TG and PL contribution in 1H NMR spectrum).

^{31}P NMR spectrum has been recorded (see figure 4.20) to obtain the composition of the phospholipids classes presents in the total lipid fraction with-

Results and discussion

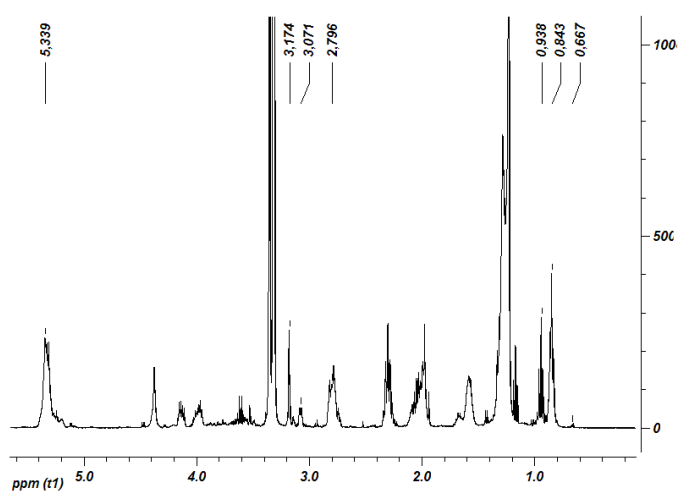


Figure 4.34: ^1H NMR spectrum of raw organic extract of *Pseudodiamesa branickii* in $\text{CDCl}_3 : \text{CD}_3\text{OD}$ 2 : 1

out interferences by triglycerides signals.

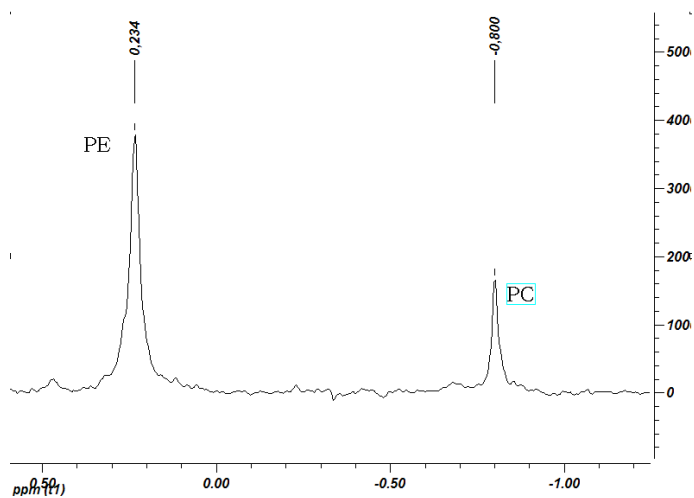


Figure 4.35: ^{31}P NMR spectrum of raw organic extract of *Pseudodiamesa branickii* in $\text{CDCl}_3 : \text{CD}_3\text{OD}$ 2 : 1

The figure 4.36 shows that also in *Pseudodiamesa branickii* are present only two classes, PC and PE, and that the predominant is PE but, with respect to *Diamesa cinerella*, the amount of PC is increased.

HPLC/ESI-MS experiments have been carried out allowing the identifi-

4.3 Cold resistance in Chironomid larvae

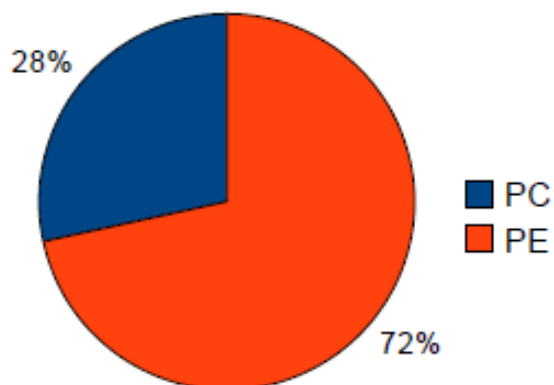


Figure 4.36: Percentage composition of *Pseudodiamesa branickii*

cation of all the fatty chains bound to these two PL classes. As shown in the figure 4.37, in the distribution of PE there are some remarkable differences between the two temperatures: at +4 °C there is a relevant domination of the species 34:3 (yellow circles), at -4 °C the species predominant are 36:5 and 36:6 (red circles).

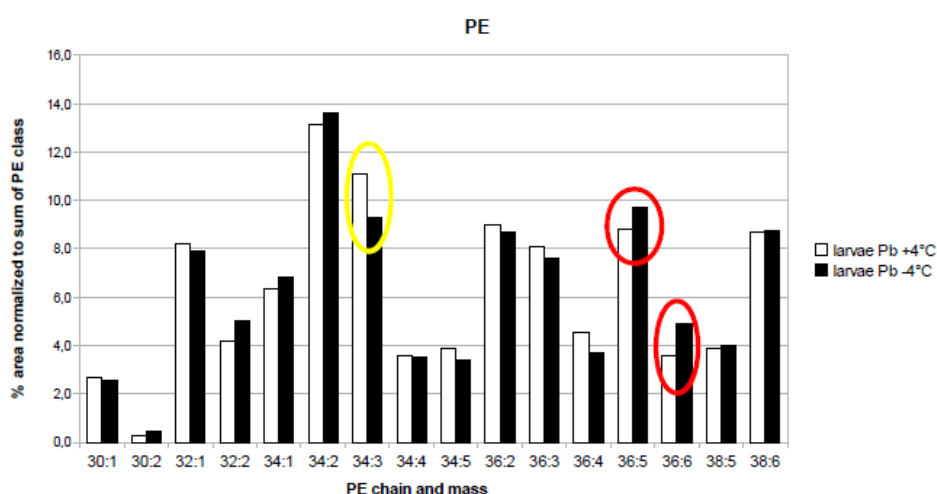


Figure 4.37: Distribution of PE in *Pseudodiamesa branickii* at +4°C and -4°C as obtained by LC-MS experiment

Results and discussion

It is possible to identify some sequences of lipids by the analysis of chains identified by ESI negative-ion mode (see table 4.4).

PE lipid	Chain 1	Chain 2
30:1	Unknown	Unknown
30:2	Unknown	Unknown
32:1	16:0	16:1
32:2	Unknown	Unknown
34:1	16:0	18:1
34:2	16:0	18:2
34:2	16:1	18:1
34:3	Unknown	Unknown
34:3	16:0	18:3
34:4	Unknown	Unknown
34:4	Unknown	Unknown
34:5	Unknown	Unknown
36:2	18:0	18:2
36:2	18:1	18:1
36:3	18:0	18:3
36:3	18:1	18:2
36:4	18:1	18:3
36:5	16:0	20:5
36:6	16:1	20:5
38:5	18:0	20:5
38:6	18:1	20:5

Table 4.4: Fatty acid chains of PE lipids from negative-ion mode ESI in *Pseudodiamesa branickii*

In PLs with 36 carbon atoms, for mono, di, tri and tetraunsaturated chains a sequence based on the couple 18:0/18:x (x=1-4) could be inferred; for chains with more than five unsaturation the presence of the 20:5 chain is a recurrent feature. Analyzing the distribution by number of carbon atoms

4.3 Cold resistance in Chironomid larvae

of fatty acid chains in figure 4.38, a little predominance at + 4°C of PLs with 34 carbon atoms and at -4°C of PLs with 36 carbon atoms is observed.

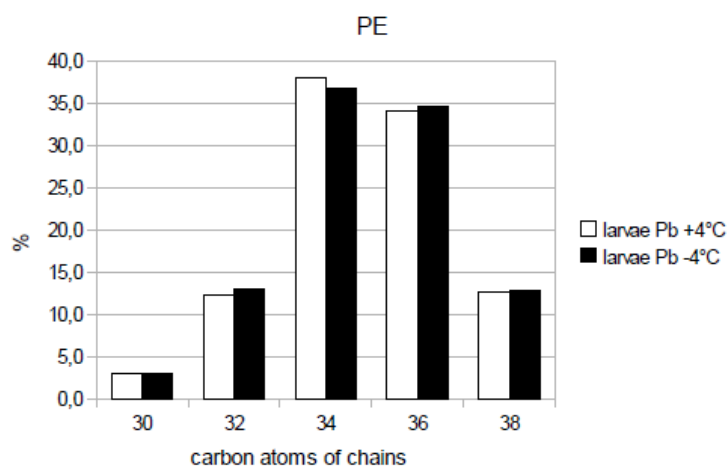


Figure 4.38: Distribution of PE divided by number of carbon atoms of the two fatty acid chains in *Pseudodiamesa branickii*

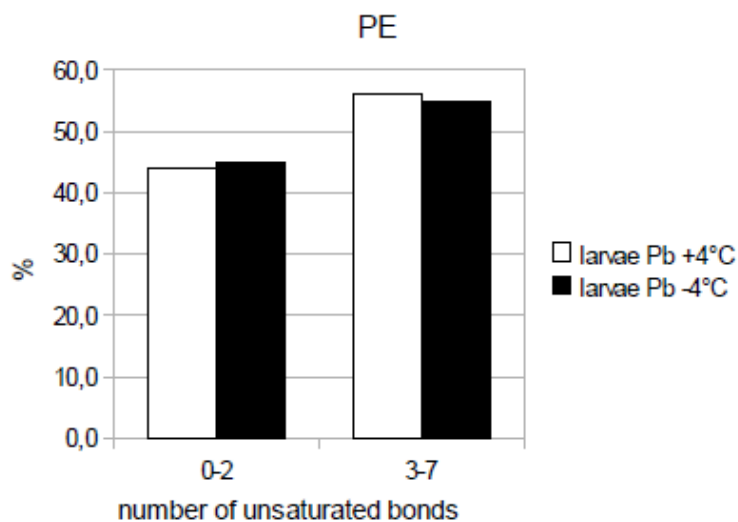


Figure 4.39: Distribution of PE divided by number of unsaturated bonds of the two fatty acid chains in *Pseudodiamesa branickii*

Results and discussion

As shown in the figure 4.40, in the distribution of PC there are some remarkable differences between the two temperatures: at +4 °C there is a relevant domination of the species 34:3 (yellow circles), at -4 °C the species predominant are 36:5 and 36:6 (red circles).

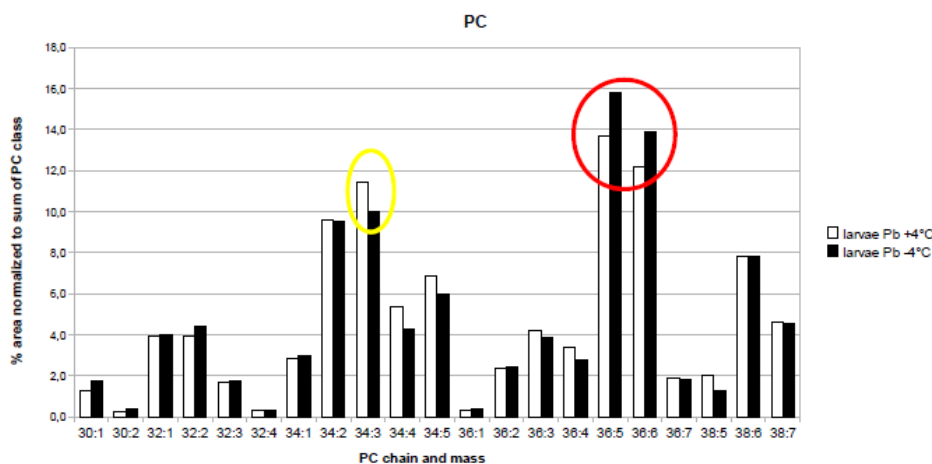


Figure 4.40: Distribution of PC in *Pseudodiamesa branickii* at +4°C and -4°C as obtained by LC-MS experiment

Analyzing the distribution by number of carbon atoms of fatty acid chains (figure 4.41), a net predominance at + 4°C of lipid with 34 carbon atoms and at -4°C of lipid with 36 carbon atoms is observed, like in *Diamesa cinerella*.

In *Pseudodiamesa branickii* the species identified as PEx and PCx have not been detected. For these extracts GC-MS measurements have not been carried out because of the low quantity of the two samples.

After observing that NMR spectrum was too crowded for allowing a reliable assignment of the various peaks, HPLC/ESI-MS experiments in positive and negative ion mode were performed to identify sugars and polyols presents in the samples and to observe if there are some significant trends with the temperature. Some sugars have been identified (glucose, sorbitol, sucrose, raffinose and lactose) but not trehalose. From +4 °C to -4 °C there is a little increase of glucose concentration and a decrease of lactose and raffinose.

4.3 Cold resistance in Chironomid larvae

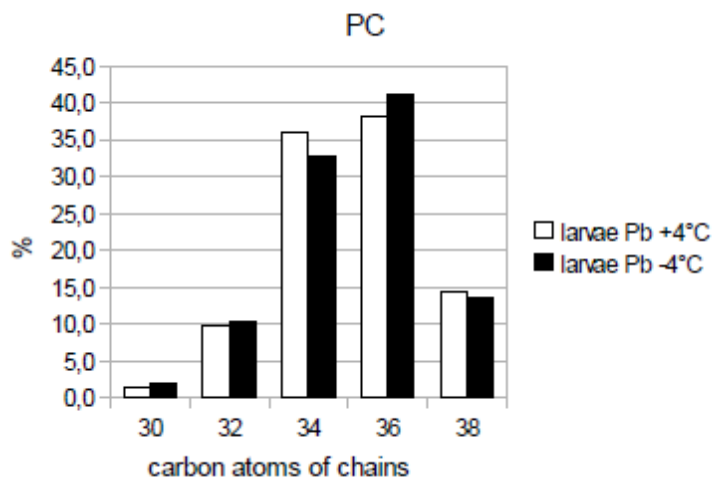


Figure 4.41: Distribution of PC divided by number of carbon atoms of the two fatty acid chains in *Pseudodiamesa branickii*

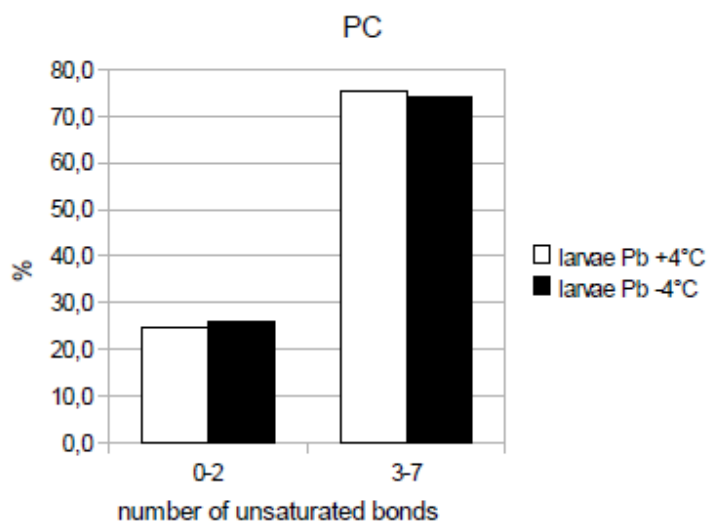


Figure 4.42: Distribution of PC divided by number of unsaturated bonds of the two fatty acid chains in *Pseudodiamesa branickii*

Results and discussion

4.3.3 Discussion

If the attention is focused only on the global trend of each class, observing the variations on the mean unsaturation index (MUI) calculated from LC-MS experiments (see table 4.5), the differences between the two temperatures are small and not particularly meaningful.

	PB +4°C	PB -4°C	DC +4°C	DC -4°C
PE	3,17	3,08	3,73	3,82
PC	4,07	4,09	4,63	4,51

Table 4.5: Mean unsaturation index of PE and PC in *Pseudodiamesa branickii* (PB) and in *Diamesa cinerella* (DC) at +4°C and -4°C obtained by LC-MS measurements

In *Diamesa cinerella* there is a little increase of PE mean unsaturation counterbalanced by a small decrease of PC mean unsaturation. In *Pseudodiamesa branickii* PC mean unsaturation have the same value and there is a small decrease of PE mean unsaturation. The counterbalance observed in *Diamesa* larvae adapted to low temperature living conditions could be interpreted as a mechanism of redistribution of acyl chains among the phospholipids rather than large changes in acyl chain unsaturation, that it has been already reported in literature for ciliates [60]. However, if the attention is focused on the variations of the relative molar ratios of each phospholipid, there are some significant differences.

The great amount of PE compared to PC has been already reported in literature and it has been correlated to the cold adaptation [61]; moreover, from MUI data it's clear that in both species PE are less unsaturated than PC, in apparent contrast to the normal behavior reported in literature [62], but in agreement with previous results reported for insects [61]. Analyzing the distribution of the total number of carbon atoms in the FA chains of PE and PC, it's clear that at the lower temperature (-4°C) there is always a small prevalence of longer chains (36 C atoms); this observation could be

4.3 Cold resistance in Chironomid larvae

explained by the more disorder produced by longer chains contributing to preserve membrane fluidity.

Comparing *Diamesa cinerella* to *Pseudodiamesa branickii*, the first observation is that the former has a greater ratio PE/PC and has a MUI value higher than the later. These two factors could be explained by the higher altitude where *Diamesa* larvae usually live with environmental conditions harder than *Pseudodiamesa* requiring stronger cold adaptation mechanisms to restore a functional membrane fluidity. One interesting fact is the widespread coupling in PL of one chain essentially saturated and short and of a second one with a significantly higher MUI and carbon atoms number. This pairing could be explained as another cold adaptation mechanism, because a similar pairing of FA chains enlarges the range of temperatures at which membranes are fluid and results in both cold and heat tolerance. This assumption is based on the finding of Lewis et al. [63] that the difference ($T_h - T_m$) between the two phase transition temperatures of PE-phospholipids (T_m for transition to gel phase and T_h for transition to inverted hexagonal phase) increases markedly with a decrease in acyl chain length. Lowering of T_m could prevent unregulated formation of gel phase at lower ambient temperatures typical for overwintering larvae. Maintaining large difference between T_m and T_h temperatures could assure that the transition to hexagonal phase in PEs does not occur in unregulated way upon a sudden increase of temperature or during dehydration upon freezing.

Our results also suggest that the concentration of PE species with a 20:5 esterified chain at sn-2 position is higher at -4°C than at $+4^{\circ}\text{C}$ (see in *Diamesa* larvae 34:5 and 36:5 PE or in *Pseudodiamesa* larvae 36:5 PE). From ESI negative-ion mode measurements on PE we have established that the main PUFA present in the fatty acid chain pattern is 20:5, with a very small percentage of 22:6. It has been demonstrated in literature that in aquatic invertebrates FA composition in phospholipids is strongly determined genetically by specific biosynthesis [64]. The main enzymes related to the lipid biosynthesis are desaturases and elongases. Fatty acid desaturases

Results and discussion

are enzymes that convert a single bond between two carbon atoms (C-C) to a double bond (C=C) in a fatty acyl chain and the distribution of these proteins is almost universal. The ability of cells to modulate the physical characteristics of their membrane lipids is determined mainly by the actions of fatty acid desaturases, which introduce double bonds into fatty acids [65]. There are three types of fatty acid desaturase: acyl-CoA, acyl-ACP, and acyl-lipid desaturases [66]. In plants and cyanobacteria, most desaturation reactions are catalyzed by acyl-lipid desaturases, which introduce unsaturated bonds into fatty acids that are bound to the glycerol moiety of polar glycerolipids [67]. Acyl-ACP desaturases are present in the plastids of plant cells and introduce the first double bond into fatty acids that are bound to acyl carrier protein (ACP). Acyl-CoA desaturases are present in animal, yeast and fungal cells, and they introduce unsaturated bonds into fatty acids that are bound to coenzyme A (CoA) [68]. The terms such as elongase system, elongase, or fatty acid chain elongation system (FACES), all refer to enzymes that are responsible for the addition of two carbon units to the carboxyl end of a fatty acid chain. In both plants and animals, the elongase system is composed of four enzymes: a condensing enzyme (β -ketoacyl CoA synthase, KCS), β -ketoacyl CoA reductase (KCR), β -hydroxyacyl CoA dehydrogenase, and trans-2-enoyl CoA reductase. Fatty acid elongation mechanism is represented in figure 4.43. In the cell, there exist multiple microsomal elongation systems with different chain length specificity.

The importance of these enzymes in restoring membrane fluidity in stress conditions has been highlighted in many studies where it has been reported that one of the first biochemical responses to the membrane rigidity is the action of desaturases to lower the membrane melting temperature [28][69]. The PUFA biosynthesis mechanisms have been elucidated [70] and they require the action of some desaturases and elongases enzymes, as described in figure 4.44.

Whereas the synthetic mechanism of eicosapentaenoic acid (20:5) is unambiguous, for docosahexanoic acid (22:6) there are two distinct mecha-

Elongation of Fatty Acid

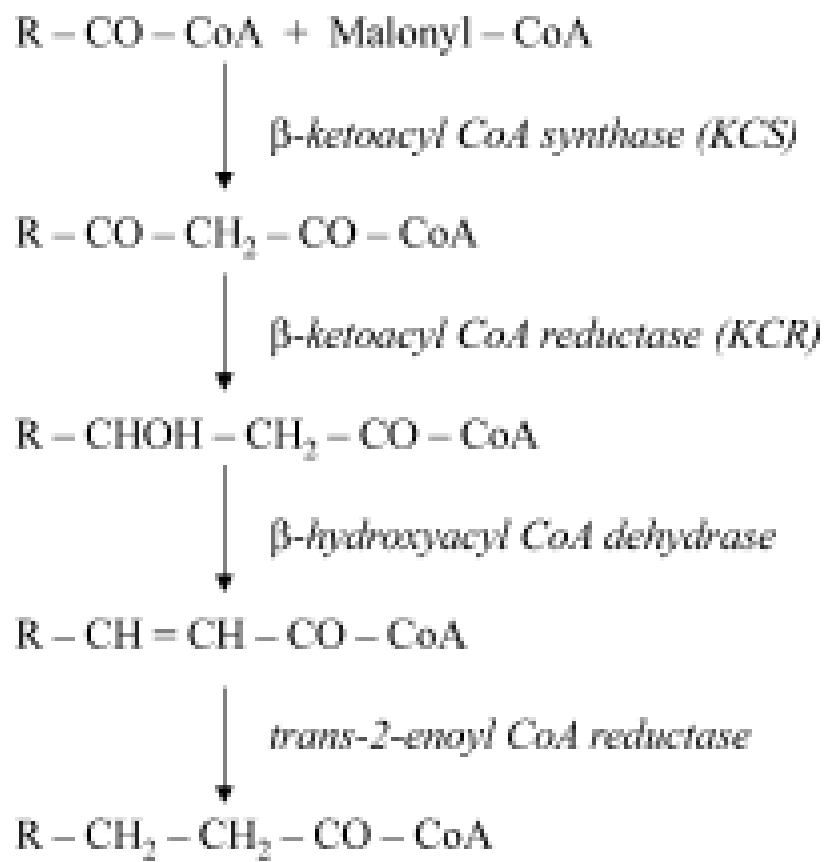


Figure 4.43: Fatty acid chain elongation reaction

Results and discussion

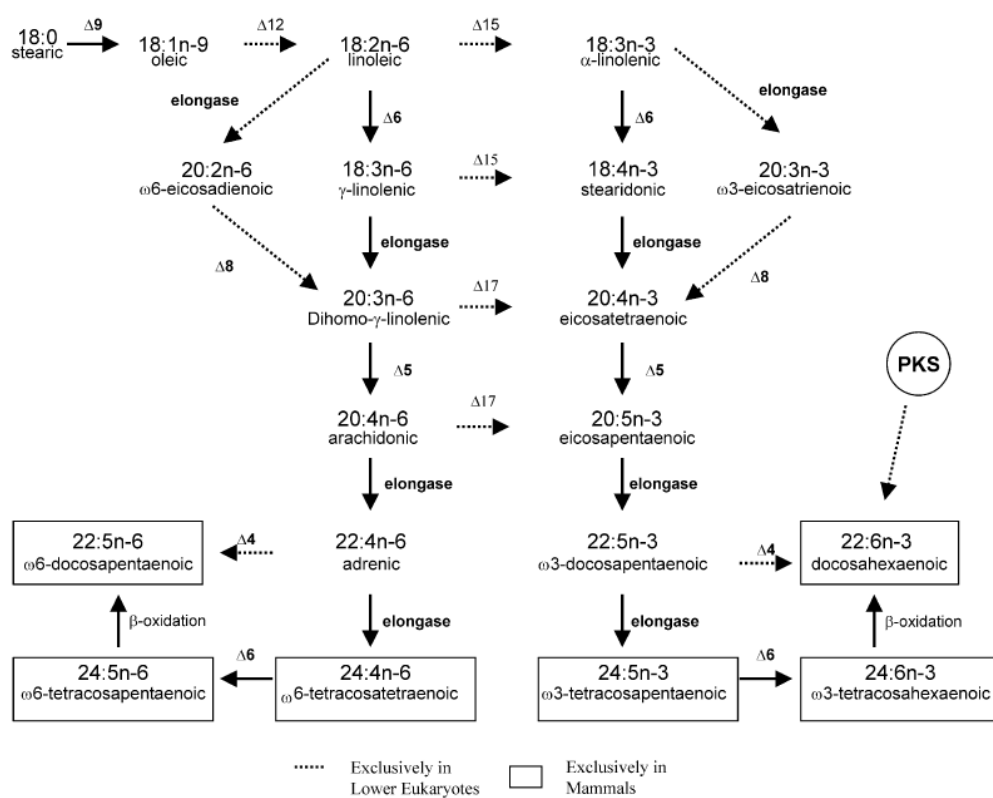


Figure 4.44: Biosynthesis of long-chain polyunsaturated fatty acids. Arrows with solid line are found both in mammals and lower eukaryotes, while arrows with dotted line are exclusively for lower eukaryotes. Fatty acids in the box indicate the pathway is exclusively in mammals. Reprinted from [70]

4.3 Cold resistance in Chironomid larvae

nisms for mammals [71] and for lower eukaryotes [72]. The cellular structures of *Diamesa cinerella* and *Pseudodiamesa branickii* are more similar to lower eukaryotes and so it could be supposed that they synthesize 22:6 through the direct action of $\Delta 4$ desaturase on 22:5 without the steps implicating the formation of 24:5 and 24:6 fatty acids but we don't have sufficient results to assert absolutely this mechanism.

The low concentration of PL with 22:6 chain esterified (there is only 36:6 PE) could be attributed to a low activity of $\Delta 4$ desaturase or to a low activity of elongases. In the past the desaturation steps have long been considered the rate-limiting steps for the biosynthesis of PUFAs, but recently studies in *M. alpina* indicate that the elongation of C18:3 ω -6 to C20:3 ω -6 is the rate-limiting step in 20:4 acid biosynthesis [73]. Another biochemical problem is the identification of the type of desaturases presents in our samples, i.e. if the desaturation process is localized in the fatty acid bound to glycerol backbone, like in cyanobacteria, or if they introduce unsaturated bonds into fatty acids that are bound to coenzyme A (CoA), like in mammals. The future perspective is the identification of desaturases present in *Diamesa cinerella* and *Pseudodiamesa branickii* trying to define the mechanism of lipid biosynthesis in these insects.

Summarizing, membrane composition is important to preserve the life of the organisms and the membrane fluidity is kept by phospholipids with an high unsaturation degree to lower the melting temperature of the membrane. Varying temperature inside their vital range (from +4°C to -4°C) we can assume a mechanism of redistribution of acyl chains among the phospholipids in the absence of large changes in acyl chain unsaturation. The pairing of chains with different length in the phospholipids is another mechanism to lower melting temperature and to preserve membrane structure from cold stress. The high ratio PE/PC, not so common in other type of organisms, is typical of cold adapted species because PEs help to preserve membrane fluidity. It remains unclear the mechanism of lipid biosynthesis in these insects to have a more descriptive comprehension of biochemical

Results and discussion

processes inside the cell, which type of desaturases are present in these organisms and if the unsaturated bonds are introduced on fatty acids bound to the glycerol moiety of polar glycerolipids or bound to coenzyme A. In a preliminary analysis, polyols and sugars don't seem to play an important role in adaptation in their vital range. Other experiments on larvae adapted at very low temperature ($< -8^{\circ}\text{C}$) or at very high temperature ($> 20^{\circ}\text{C}$) could be useful to have a description of stress response in *Diamesa cinerella* and *Pseudodiamesa branickii*.

Chapter 5

Conclusions

The aim of this study was to investigate biological membranes and to demonstrate how the knowledge about their composition can be useful to understand the biochemical processes involved in the response to environmental stressors or diseases and the great relevance that lipidomics can play in this context. The study has been focused on two specific biological systems: *i)* the components of DRM (detergent resistant membrane) associated with the expression of PSMA, a protein involved in the prostate carcinoma and *ii)* the composition of membranes of insect larvae of two species (*Pseudodiamesa branickii* and *Diamesa cinerella*) to obtain a better understanding of the mechanisms involved in the adaptation of the organisms at temperature below 0°C.

From the analysis of components of DRMs our investigations outline the mild "extracting power" of Lubrol which leads to rafts with a low ratio Chol/PL respect to other stronger detergents, like Triton X-100, with a lower SM/PC and higher PE/PC ratios with PE representing almost 50% of the total PL in the membrane. Furthermore this study has strengthened the importance of cholesterol to trigger rafts formation and it is in agreement with the model that lipid raft stability is provided by acyl chains structure and their interaction with cholesterol.

Concerning the study on *Pseudodiamesa branickii* and *Diamesa cine-*

Conclusions

rella, our results underline the high unsaturation degree of fatty acid chains that has been related to mechanisms adopted to decrease the membrane melting temperature. By lowering temperature inside their vital range (from +4 °C to -4 °C) this species seems able to activate a mechanism of redistribution of PL acyl chains. In particular, PLs bearing acyl chains of different length are expected to be more disordered than "symmetric" PLs and, thus better-suited to tackle cold stress adaptation. Another interesting outcome is the high molar ratio of PE, a factor which seem to enhance membrane fluidity at low temperature. Polyols and sugars, molecules with well-known cryoprotective role, in a preliminary analysis don't seem to have a significant role in temperature adaptation of these insects. Two questions are left unresolved: the lipid biosynthetic mechanisms and the modification of cellular membrane in response to hot stresses. The first is important to complete the comprehension of biochemical processes involved in cold adaptation, to know which type of desaturases are present in these insects, how polyunsaturated lipids are synthesized and if the unsaturated bonds are introduced on fatty acids bound to the glycerol moiety of polar glycerolipids or bound to coenzyme A. The second question is relevant in an ecological perspective to understand how these organisms respond to the increase of environmental temperature and if they are able to survive the global warming.

Bibliography

- [1] Domon B and Aebersold R., Review - Mass spectrometry and protein analysis, *Science*,2006, **312**, 212; Sickmann A., Mreyen M. and Meyer H.E., Mass spectrometry - a key technology in proteom research, *Adv. Biochem. Eng. Biotechnol.*,2003, **83**, 141.
- [2] Goodacre R., Vaidyanathan S., Dunn W.B., Harrigan G.G. and Kell D.B., Metabolomics by numbers: acquiring and understanding global metabolic data, *Trends Biotechnol.*,2004, **22**, 245
- [3] Wenk M.R., The emerging field of lipidomics, *Nat. Rev. Drug. Discov.*,2005, **4**, 594.
- [4] Oresic M., Hänninen V.A. and Vidal-Puig A., Lipidomics: a new window to biomedical frontiers, *Trends Biotechnol.*,2008, **26**, 647-652
- [5] Fahy E., Subramaniam S., Brown H.A., Glass C.K., Merrill A.H., Murphy R.C., Raetz C.R.H., Russell D.W., Seyama Y., Shaw W., Shimizu T., Spener F., van Meer G., VanNieuwenhze M.S., White S.H., Witztum J.L. and Dennis E.A., A comprehensive classification system for lipids, *J. Lipid Res.*,2005, **46**, 839-861
- [6] Pulfer M. and Murphy R.C., Electrospray mass spectrometry of phospholipids, *Mass Spectrom. Rev.*,2003, **22**, 332-364
- [7] Schiller J., Suss R., Arnhold J., Fuchs B., Lessig J., Muller M., Petkovic M., Spalteholz H., Zschornig O. and Arnold K., Matrix-assisted laser

BIBLIOGRAPHY

- desorption and ionization time-of-flight (MALDI-TOF) mass spectrometry in lipid and phospholipid research, *Prog. Lipid Res.*,2004, **43**, 449-488
- [8] Ejsing C.S., Sampaio J.L., Surendranath V., Duchoslav E., Ekroos K., Klemm R.W., Simons K. and Shevchenko A., Global analysis of the yeast lipidome by quantitative shotgun mass spectrometry, *Proc. Natl. Acad. Sci. U.S.A.*,2009, **106**, 2136
- [9] Deeley J.M., Hankin J.A., Friedrich M.G., Murphy R.C., Truscott R.J.W., Mitchell T.W. and Blanksby S.J., Sphingolipid distribution changes with age in the human lens, *J. Lipid Res.*,2010, **51**, 2753-2760
- [10] Koivusalo M., Perttu Haimi P., Heikinheimo L., Kostianen R. and Somerharju P., Quantitative determination of phospholipid compositions by ESI-MS: effects of acyl chain length, unsaturation, and lipid concentration on instrument response, *J. Lipid Res.*,2001, **42**, 663-672
- [11] Taleb A., Diamond J., McGarvey J.J., Beattie J.R., Toland C. and Hamilton P.W., Raman microscopy for the chemiometric analysis of tumor cells, *J. Phys. Chem. B*,2006, **110**, 19625-19631
- [12] Singer S.J. and Nicolson G.L., The fluid mosaic model of the structure of cell membranes, *Science*,1972, **175**, 720-731
- [13] Van Meer G., Lipid traffic in animal-cells, *Annu. Rev. Cell. Biol.*,1989, **5**, 247
- [14] Simons K. and Ikonen E., Functional rafts in cell membranes, *Nature*,1997, **387**, 569-572
- [15] Brown D.A. and London E., Structure and origin of ordered lipid domains in biological membranes, *J. Membr. Biol.*,1998, **164**, 103-114

BIBLIOGRAPHY

- [16] Brown D.A. and Rose J., Sorting of GPI-anchored proteins to glycolipid-enriched membrane subdomains during transport to the apical cell-surface, *Cell*,1992, **68**, 533-544
- [17] Schuck S., Honsho M., Ekroos K., Shevchenko A. and Simons K., Resistance of cell membranes to different detergents, *Proc. Natl. Acad. Sci. U.S.A.*,2003, **100**, 5795-5800
- [18] Niemelä P.S., Ollila S., Hyvönen M.T., Karttunen M. and Vattulainen I., Assessing the nature of lipid raft membranes, *PLOS Comput. Biol.*,2007, **3**, 304-312; Edidin M., The state of lipid rafts: From model membranes to cells, *Annu. Rev. Biophys. Biomolec. Struct.*,2003, **32**, 257-283
- [19] Samsonov A.V., Mihalyov I. and Cohen F.S., Characterization of cholesterol-sphingomyelin domains and their dynamics in bilayer membranes, *Biophys. J.*,2001, **81**, 1486-1500
- [20] Schmidt C.F., Barenholz Y. and Thompson T.E., Nuclear Magnetic-resonance study of sphingomyelin in bilayer systems, *Biochemistry*, 1977, **16**, 2649-2656
- [21] Boggs J.M., Intermolecular hydrogen bonding between lipids: influence on organization and function of lipids in membranes, *Can. J. Biochem.*, 1980, **58**, 755-770
- [22] Simons K. and van Meer G., Lipid sorting in epithelial cells, *Biochemistry*, 1988, **27**, 6197-6202
- [23] Brown D.A. and London E., Structure and Function of Sphingolipid- and Cholesterol-rich Membrane Rafts, *J. Biol. Chem.*,2000, **275**, 17221-17224
- [24] London E. and Brown D.A., Insolubility of lipids in Triton X-100: physical origin and relationship to sphingolipid/cholesterol membrane domains (rafts), *Biochim. Biophys. Acta*,2000, **1508**, 182-195

BIBLIOGRAPHY

- [25] Castelletti D., Alfalah M., Heine M., Hein Z., Schmitte R., Fracasso G., Colombatti M. and Naim H.Y., Different glycoforms of prostate-specific membrane antigen are intracellularly transported through their association with distinct detergent-resistant membranes, *Biochem. J.*,2008, **409**, 149-157
- [26] Landers K.A., Burger M.J., Tebay M.A., Purdie D.M., Scells B., Samarasingha H., Lavin M.F. and Gardiner R.A., Use of multiple biomarkers for a molecular diagnosis of prostate cancer, *Int. J. Cancer*,2005, **114**, 950-956
- [27] Israeli R.S., Powell C.T., Corr J.G., Fair W.R. and Heston W.D., Expression of the prostate-specific membrane antigen, *Cancer Res.*,1994, **54**, 1807-1811
- [28] Los D.A. and Murata N., Membrane fluidity and its roles in the perception of environmental signals, *Biochim. Biophys. Acta*,2004, **1666**, 142-157
- [29] Wang G., Shusen L., Hainan L., Brumbaugh E.E. and Huang C., Effects of various numbers and positions of cis double bonds in the sn-2 acyl chain of phosphatidylethanolamine on the chain-melting temperature, *J. Biol. Chem.*,1999, **274**, 12289-12299
- [30] Keough, K. M. W., Influence of chain unsaturation and chain position on thermotropism and intermolecular interactions in membranes, *Biochem. Soc. Trans.*,1990, **18**, 835-837
- [31] Huang C., Hainan L., Shusen L. and Wang G., Influence of the positions of cis double bonds in the sn-2 acyl chain of phosphatidylethanolamine on the bilayer's melting behavior, *J. Biol. Chem.*,1997, **272**, 21917-21926

BIBLIOGRAPHY

- [32] Watanabe M., Kikawada T. and Okuda T., Increase of internal ion concentration triggers trehalose synthesis associated to cryptobiosis in larvae of *Polypedilum vanderplanki*, *J. Exp. Biol.*,2003, **206**, 2281-2286
- [33] Behm C.A., The role of trehalose in the physiology of nematodes, *Int. J. Parasit.*,1997, **27**, 215-229
- [34] Schulze U., Larsen M.E. and Villadsen J., Determination of intracellular trehalose and glycogen in *Saccharomyces cerevisiae*, *Anal. Biochem.*,1995, **228**, 143-149
- [35] Sum A.K., Faller R. and de Pablo J.J., Molecular simulation study of phospholipid bilayers and insights of the interactions with disaccharides, *Biophys. J.*,2003, **85**, 2830-2844
- [36] Crowe J.H., Crowe L.M. and Chapman D., Preservation of membranes in anhydrobiotic organisms - the role of trehalose, *Science*,1984, **223**, 701-703
- [37] Lencioni V., Survival strategies of freshwater insects in cold environments, *J. Limnol.*,2004, **63(Suppl.1)**, 45
- [38] Bouchard R.W., Carrillo M.A., Kells S.A. and Ferrington L.C., Freeze tolerance in larvae of the winter-active *Diamesa mendotae* Muttkowski (Diptera : Chironomidae): a contrast to adult strategy for survival at low temperatures, *Hydrobiologia*,2006, **568**, 403-416; Rossaro, B. Chironomids and water temperature, *Aquatic Insects*,1991, **13**, 87-98; Lencioni V. and Rossaro B., Microdistribution of chironomids (Diptera: Chironomidae) in Alpine streams: an autoecological perspective, *Hydrobiologia*,2005, **533**, 61-76
- [39] Michaud M.B., Benoit J.B., Lopez-Martinez G., Elnitsky M.A., Lee R.E. and Denlinger D.L., Metabolomics reveals unique and shared metabolic changes in response to heat shock, freezing and desiccation in the

BIBLIOGRAPHY

- Antarctic midge, *Belgica antarctica*, *J. Insect Physiol.*,2008, **54**, 645-655
- [40] Benoit J.B., Lopez-Martinez G., Elnitsky M.A., Lee R.E. and Denlinger D.L., Dehydration-induced cross tolerance of *Belgica antarctica* larvae to cold and heat is facilitated by trehalose accumulation, *Comp. Biochem. Physiol. A*,2009, **152**, 518-523
- [41] Hopfgartner G., Vilbois F. and Piguet C., Characterization of supramolecular complexes by high resolution electrospray ionization mass spectrometry, *Rapid Commun. Mass Spectrom.*,1999, **13**, 302-306
- [42] Pitt A.R., Application of electrospray mass spectrometry in biology, *Nat. Prod. Rep.*,1998, **15**, 59-72
- [43] Yamashita M. and Fenn J.B., Electrospray ion-source - another variation on the free-jet theme, *J. Phys. Chem.*,1984, **88**, 4451-4459
- [44] Iribarne J.V. and Thomson B.A., On the evaporation of small ions from charged droplets, *J. Chem. Phys.*,1976, **64**, 2287
- [45] Dole M., Mack L.L., Hines R.L., Mobley R.C., Ferguson L.D. and Alice M.B., Molecular beams of macroions, *J. Chem. Phys.*,1968, **49**, 2240
- [46] Kerwin J.L., Tuininga A.R. and Ericsson L.H., Identification of molecular-species of glycerophospholipids and sphingomyelin using electrospray mass-spectrometry, *J. Lipid Res.*,1994, **35**, 1102-1114
- [47] Bligh E.G. and Dyer W.J. , A rapid method of total lipid extraction and purification, *Can. J. Biochem. Physiol.*,1959, **37**, 911-917
- [48] Folch J., Lees M. and Stanley G.H.S., A simple method for the isolation and purification of total lipides from animal tissues, *J. Biol. Chem.*,1957, **226**, 497-509

BIBLIOGRAPHY

- [49] Dennis A. and Plückthun A., Phosphorus-31 NMR of Phospholipids in Micelles, in Phosphorus-31 NMR - Principles and Applications, Gorenstein editor, Orlando Academic Press Inc, 1984, 423-446
- [50] Schiller J., Muller M., Fuchs B., Arnold K. and Huster D., P-31 NMR Spectroscopy of phospholipids: from micelles to membranes, *Curr. Anal. Chem.*, 2007, **3**, 283-301; Schiller J. and Arnold K., Application of high resolution ^{31}P NMR spectroscopy to the characterization of the phospholipid composition of tissues and body fluids - a methodological review, *Med. Sci. Monitor*, 2002, **8**, 205-222
- [51] London E. and Feigenson G.W., Phosphorus NMR analysis of phospholipids in detergents *J. Lipid Res.*, 1979, **20**, 408-412
- [52] Meneses P. and Glonek T., High resolution ^{31}P NMR of extracted phospholipids, *J. Lipid Res.*, 1988, **29**, 679-689; Bosco M., Culeddu N., Toffanin R. and Pollesello P., Organic Solvent Systems for ^{31}P Nuclear Magnetic Resonance Analysis of Lecithin Phospholipids: Applications to Two-Dimensional Gradient-Enhanced ^1H -Detected Heteronuclear Multiple Quantum Coherence Experiments, *Anal. Biochem.*, 1997, **245**, 38-47; Culeddu N., Bosco M., Toffanin R. and Pollesello P., ^{31}P NMR analysis of phospholipids in crude extracts from different sources: improved efficiency of the solvent system, *Magn. Reson. Chem.*, 1998, **36**, 907-912
- [53] Hao L., Lu R.H., Leaist D.G. and Poulin P.R., Aggregation number of aqueous sodium cholate micelles from mutual diffusion measurements, *J. Solut. Chem.*, 1997, **26**, 113-125
- [54] Brzustowicz M.R., Cherezov V., Zerouga M., Caffrey M., Stillwell W. and Wassall S.R., Controlling membrane cholesterol content. A role for polyunsaturated (Docosahexaenoate) phospholipids, *Biochemistry*, 2002, **41**, 12509-12519

BIBLIOGRAPHY

- [55] Shaikh S.R., Cherezov V., Caffrey M., Stillwell W. and Wassall S.R., Interaction of cholesterol with a docosahexaenoic acid-containing phosphatidylethanolamine: Trigger for microdomain/raft formation?, *Biochemistry*, 2003, **42**, 12028-12037
- [56] Košťal V., Berkova P. and Šimek P., Remodelling of membrane phospholipids during transition to diapause and cold-acclimation in the larvae of *Chymomyza costata* (Drosophilidae), *Comp. Biochem. Physiol. B*, 2003, **135**, 407-419
- [57] Martinez-Seara H., Rog T., Karttunen M., Vattulainen I. and Reigada R., Why is the sn-2 chain of monounsaturated glycerophospholipids usually unsaturated whereas the sn-1 chain is saturated? Studies of 1-stearoyl-2-oleoyl-sn-glycero-3-phosphatidylcholine (SOPC) and 1-oleoyl-2-stearoyl-sn-glycero-3-phosphatidylcholine (OSPC) membranes with and without cholesterol, *J. Phys. Chem. B*, 2009, **113**, 8347-8356
- [58] Lie Ken M.S.F. and Lam C.C., ¹H Nuclear magnetic resonance spectroscopic studies of saturated, acetylenic and ethylenic triacylglycerols, *Chem. Phys. Lipids*, 1995, **77**, 155-171
- [59] Gao J., Ajjawi I., Manoli A., Sawin A., Xu C., Froehlich J.E., Last R.L. and Benning C., FATTY ACID DESATURASE4 of Arabidopsis encodes a protein distinct from characterized fatty acid desaturases, *Plant J.*, 2009, **60**, 832-839
- [60] Dickens, B.F. and Thompson, G.A., Phospholipid molecular species alterations in microsomal membranes as an initial key step during cellular acclimation to low temperature, *Biochemistry*, 1982, **21**, 3604-3611
- [61] Hodkova, N. Šimek P., Zahradničkova H. and Novakova O., Seasonal changes in the phospholipid composition in thoracic muscles of a heteropteran, *Pyrrhocoris apterus*, *Insect Biochem. Mol. Biol.*, 1999, **29**, 367-376

BIBLIOGRAPHY

- [62] Hazel, J.R., Cold adaptation in ectotherms: regulation of membrane function and cellular metabolism. *Adv. Comp. Environ. Physiol.*,1989, **4**, 1-49
- [63] Lewis, R.N.A.H., Mannock D.A., McElhaney R.N., Turner D.C. and Gruner S.M., Effect of fatty acyl chain length and structure on the lamellar gel to liquidcrystalline and lamellar to reversed hexagonal phase transition of aqueous phosphatidylethanolamine dispersions, *Biochemistry*, 1989, **28**, 541-548
- [64] Falk-Petersen S., Sargent J.R., Kwasniewski S., Gulliksen B. and Millar R.M., Lipids and fatty acids in *Clione limacina* and *Limacina helicina* in Svalbard waters and the Arctic Ocean: trophic implications, *Polar Biol.*,2001, **24**, 163-170
- [65] Kates M. and Manson L.A., Regulation of membrane fluidity by lipid desaturases, *Biomembranes*,1984, **12**, 379-395
- [66] Murata N. and Wada H., Acyl-lipid desaturases and their importance in the tolerance and acclimatization to cold of cyanobacteria, *Biochem. J.*,1995, **308**, 1-8
- [67] Murata N., Wada H.and Gombos Z., Modes of fatty-acid desaturation in cyanobacteria, *Plant Cell Physiol.*,1992, **33**, 933-941
- [68] Macartney A., Maresca B and Cossins A.R., Acyl-CoA desaturases and the adaptive regulation of membrane lipid composition, in: A.R. Cossins (Ed.), Temperature adaptation of biological membranes, Portland Press, London, 1994, pp. 129-139
- [69] Sakamoto T. and Murata N., Regulation of the desaturation of fatty acids and its role in tolerance to cold and salt stress, *Curr. Opin. Microbiol.*, 2002, **5**, 206-210; Aguilera J., Randez-Gil F. and Prieto J.A., Cold response in *Saccharomyces cerevisiae*: new functions for old mechanisms, *FEMS Microbiol. Rev.*,2007, **31** 327-341

BIBLIOGRAPHY

- [70] Leonard A.E., Pereira S.L., Sprecher H. and Huang Y., Elongation of long-chain fatty acids, *Prog. Lipid Res.*,2004, **43**, 36-54
- [71] Sprecher H., Metabolism of highly unsaturated n-3 and n-6 fatty acids, *Biochim. Biophys. Acta*,2000, **1486**, 219-231
- [72] Pereira, S.L., Leonard A.E. and Mukerji P., Recent advances in the study of fatty acid desaturases from animals and lower eukaryotes, *Prostaglandins Leukot. Essent. Fatty Acids*,2003, **68**, 97-106
- [73] Wynn J.P. and Ratledge C., Evidence that the rate-limiting step for the biosynthesis of arachidonic acid in *Mortierella alpina* is at the level of the 18:3 to 20:3 elongase, *Microbiol.*,2000, **146**, 2325-2331

Acknowledgments

First of all, I convey my gratitude to my supervisor Prof. Graziano Guella for giving me the opportunity to work in his group. I am grateful for his patience and immense knowledge that have been a very precious help during all the PhD period.

The part of this thesis on DRMs has done in collaboration with dr. Mauro Dalla Serra and dr. Rossella Tomazzoli (CNR-IBF) and in collaboration with dr. Marco Colombati (University of Verona). They have taken care of all the biological part, from the cell growth to the membrane isolation.

The part of this thesis on chironomid larvae has been co-funded by the Autonomous Province of Trento (Italy), ACE-SAP project (Ecosistemi Alpini e Cambiamento Ambientale: Sensibilità e Potenziale Adattativo della biodiversità/ Alpine Ecosystems in A Changing Environment: Biodiversity Sensitivity And Adaptive Potential; regulation number 23, June 12th 2008, of the University and Scientific Research Service). I thank to dr. Valeria Lencioni (MTSN), as coordinator of the workpackage 3 activity 2, for the advices during the research and for the help in the revision of the thesis, and dr. Paola Bernabò and dr. Luigi Caputi (MTSN-CIBIO) for larvae collection and stressing experiments.

I thank to Adriano Sterni for LC-MS experiments. I thank to Lorenza Conterno for English revision of the thesis. I am grateful to Andrea, Rita and Giorgina for their initial welcome, for all lunches shared in these three years, for all the discussions and exchange of ideas.

Last but not least, I must thank very much to my parents for giving me

BIBLIOGRAPHY

support and for being always a safe haven.

List of publications

1. Toffoletti A., Conti F., Sandron T., Napolitano A., Panzella L. and D'Ischia M., Time-resolved EPR observation of synthetic eumelanin-superoxide radical pairs, *Chem. Comm.*, 2009, **33**, 4977-4979

2. Guella G., Frassanito R., Mancini I., Sandron T., Modeo L., Verni F., Dini F. and Petroni G., Keronopsamides, a New Class of Pigments from Marine Ciliates, *Eur. J. Org. Chem.*, 2010, **3**, 427-434